

Bio-Inspired Adaptive Cooperative Control of Heterogeneous Robotic Networks

Insu Chang* and Soon-Jo Chung†

University of Illinois at Urbana-Champaign, Urbana, IL 61801

We introduce a new adaptive cooperative control strategy for robotic networks comprised of heterogeneous members. The proposed feedback synchronization exploits an active parameter adaptation strategy as opposed to adaptive parameter estimation of adaptive control theory. Multiple heterogeneous robots or vehicles can coordinate their motions by parameter adaptation analogous to bio-genetic mutation and adaptation. In contrast with fixed gains used by consensus theory, both the tracking control and diffusive coupling gains are automatically computed based on the adaptation law, the synchronization errors, and the tracking errors of heterogeneous robots. The optimality of the proposed adaptive cooperative control is studied via inverse optimal control theory. The proposed adaptive cooperative control can be applied to any network structure. The stability proof, by using a relatively new nonlinear stability tool, contraction theory, shows globally asymptotically synchronized motion of a heterogeneous robotic network. This adaptive cooperative control can be widely applied to cooperative control of unmanned aerial vehicles (UAVs), formation flying spacecraft, and multi-robot systems. Results of the simulation show the effectiveness of the proposed adaptive cooperative control laws especially for a network comprised of heterogeneous members.

I. Introduction

Distributed coordination of robotic networks has been a topic of extensive research in recent years due to its merits such as more a flexible mission design, lower cost, less development time than a single complex robot. Recent advances in computation and communication technology further stimulated the growth in the field with broader applications such as unmanned aerial vehicles (UAVs),^{28,32} spacecraft formation flying,^{2,3} autonomous underwater vehicles (AUVs),²⁷ and multi-robot systems networks.⁷ Often times, cooperative control systems require mutual synchronization of multiple motions and tasks. Synchronization is important when the network system is faced with internal or external disturbances, while uncoupled trajectory tracking control hardly achieves a good performance in synchronization in the presence of such disturbances.

Most prior works studied robotic networks comprised of identical members with fixed coupling gains and network topology. In contrast, we introduce a new adaptive cooperative control law for the distributed coordination of heterogeneous robotic networks. The objective is to derive a unified synchronization framework for a heterogeneous robotic network that can achieve not only synchronization of the configuration variables of each robot but also stable tracking of a shared desired trajectory.

A. Biological Inspiration

The proposed cooperative control scheme is based on active parameter adaptation which systematically permits an active variation of physical or non-physical parameters of robotic systems. The key idea is inspired by (1) bio-genetic mutation and adaptation such as “adaptive” bio-immune systems (e.g. cytotoxic T cells)²³ and (2) Human Immunodeficiency Virus (HIV).¹⁴ For example, the cytotoxic T cell, a type of white blood cells that play a key role in the immune system and is at the core of adaptive immunity,¹ shown in Figure 1, is activated by cytokines, small proteins secreted by CD4 T cells (helper T cells). They have a

*Ph.D. Student, Department of Aerospace Engineering; chang162@illinois.edu. Student Member AIAA.

†Assistant Professor, Department of Aerospace engineering; sjchung@illinois.edu. Senior Member AIAA.

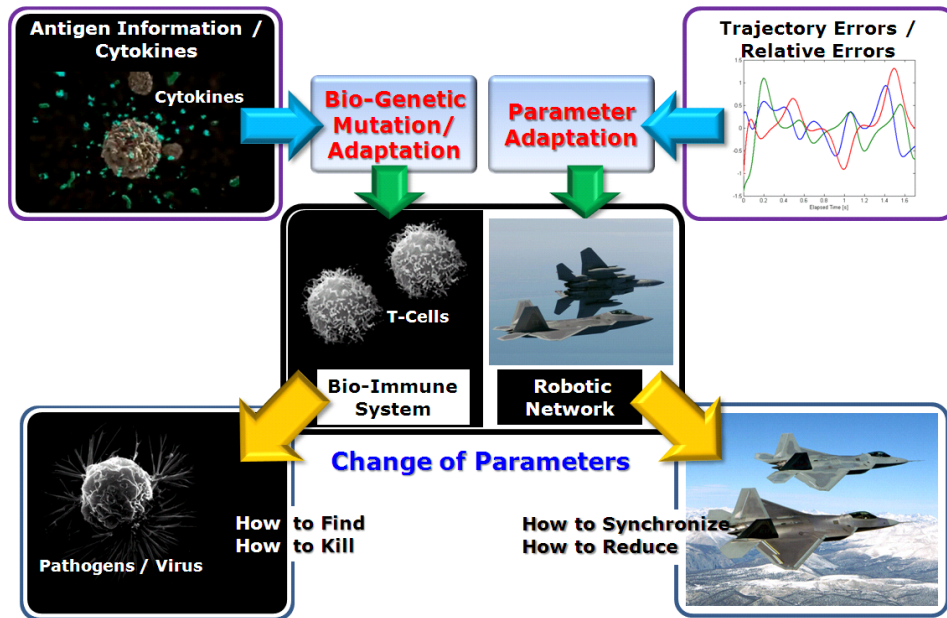


Image courtesy: Nucleus (cytokines) [<http://nucleusinc.com>], LiveScience (pathogen) [<http://www.livescience.com>], P. Groscurth (T-Cell) [Institute of Anatomy, Univ. of Zurich, Switzerland], and USAF (F-22).

Figure 1. Motivation of the current study (bio-immune system) and the relationship between the bio-immune system and systems’s dynamic motion of robotic networks

specific effect on the interactions/communications between cells. The activated T cells change their chemical and physical parameters, so that the changed parameters help the T Cells recognize their target (pathogens or tumors) in the organ. Such recognition of the adaptive immune system is a result of an adaptive biological process. It should be noted that the activated T Cells do not know where their targets are located; they only know the target’s information due to the adaptive activation process. By means of this process, the T Cells can detect their targets when they are moving around the organ. Therefore, the changed parameters in the T Cells play a crucial role in how to find and how to kill the targets. Another example is Human Immunodeficiency Virus (HIV). HIV rapidly changes its physical and biological information, so that even the adaptive bio-immune systems cannot detect the current characteristics of the virus. This procedure is different from that of the adaptive bio-immune systems. Nonetheless, the underlying concept is still the same; HIV tries to find how to avoid the T cells by changing their own physical and chemical information. These mutation and adaptation of the biological systems can be explained by a selective advantage.¹⁸ In other words, one species’ adaptation of the information can be affected by the neighbors around it.

In the current paper, we present a control-theoretic interpretation of such biological mutation and adaptation by presenting the synchronization of multiple adaptive dynamics that attempt to mimic the physical parameters of the leader. Such a leader is referred to as a knowledge leader of the adaptive network, first introduced by Wang and Slotine,³¹ which is analogous to evolutionary mutations of biological entities. This knowledge leader specifies “how to go,” as opposed to the desired trajectory prescribing “where to go.” The physical parameters that can be actively adapted include the local control gains, mass, and moments of inertia by grabbing or discarding an object or perhaps by combining or dividing the robots (e.g., autonomous docking of space robots).

B. Related Work

There has been a large volume of research on cooperative control. Detailed information can be found in the recent survey papers.^{16,20} Most prior works are based on graph theory and Laplacian [7,8,11,15,19,22]. Some of these studies use the average of the initial conditions for synchronization, which is not directly applicable to multi-robot systems whose desired trajectories are explicitly defined. Further, many prior works do not consider highly nonlinear systems such as Lagrangian dynamics, let alone the heterogeneity of a network.

We focus on adaptive control as one of the methods for synchronization of cooperative motion in robotic

networks similar to [4,6,21,29,30]. A previous study [30] applies adaptive and robust controls for cooperative manipulations in the robotic motion. However, the adaptive control is used for parameter uncertainties of the system parameters and is not applied for synchronization itself. Also, some studies [21, 29] suggest adaptive synchronization of multiple parallel manipulators in a single local coupling configuration. However, the work is also limited to the use of adaptive control that only adapts to unknown system parameters. A recent work⁴ suggests adaptive synchronization of a robotic network by estimating unknown parameters in a decentralized fashion. Most prior works focus on estimation of the system parameters by using adaptive control, while our proposed control employs adaptive control for estimating the system parameters as well as adapting them.

The main contribution of the current paper lies in the active parameter adaptation architecture for robotic networks consisting of highly nonlinear heterogeneous Lagrangian systems. The heterogeneous dynamic model presents a more generalized setup. Moreover, we introduce a novel strategy of applying the parameter adaptation to tuning both tracking control and diffusive coupling gains in an adaptive fashion. The proposed strategy aims to provide optimality as well as flexibility for highly time-varying robotic networks. The proposed parameter adaption for tracking control and diffusive coupling gains varies with system states, actuator performance, interaction with neighboring robots in the network. Unlike the prior work,⁴ the tracking control and diffusive coupling gains of each robot need not be the same for all other robots in the networks (e.g., consider formation controls of heterogeneous systems). Besides, if the agents' physical or non-physical parameters should be changed intentionally for specific missions such as docking and dividing two space robots or if they are varied by unknown environmental factors, the tracking control and diffusive coupling gains should be automatically modified as well in order to avoid a degradation in control performance.

The organization of the current paper is as follows. In Section II, modeling, general control law for tracking robotic motion, synchronization with adaptive parameter estimation, and adaptive dynamics are discussed. The synchronization of heterogeneous robotic network systems with the physical parameter adaptation is presented along with an alternative synchronization method for adaptive dynamics in section III. In section IV, main results for the current study are described. Simulation results are illustrated in section V. Finally, in section VI, the concluding remarks are stated.

II. Preliminaries: Control and Stability Analysis

We here review our main nonlinear stability tool and dynamic modeling of heterogeneous robots. Also, we summarize how a conventional adaptive controller can be applied to a robotic network. The equations of motion for a robot with multiple degrees of freedom ($\mathbf{q}_i \in \mathcal{R}^n$) can be written as:

$$\mathbf{M}_i(\mathbf{q}_i)\ddot{\mathbf{q}}_i + \mathbf{C}_i(\mathbf{q}_i, \dot{\mathbf{q}}_i)\dot{\mathbf{q}}_i + \mathbf{g}_i(\mathbf{q}_i) = \tau_i \quad (1)$$

where i ($1 \leq i \leq p$) denotes the index of robots or dynamic systems in a network, and p denotes the total number of the individual elements. In addition, τ_i is a generalized force or torque acting on the i -th system. Note that $\mathbf{C}_i(\mathbf{q}_i, \dot{\mathbf{q}}_i)$ is defined such that $(\dot{\mathbf{M}}_i - 2\mathbf{C}_i)$ is skew-symmetric,²⁵ and this property plays a central role in our stability analysis using contraction theory.¹²

A. Contraction Analysis for Global and Exponential Stability

A brief review of the contraction analysis is described in this section (see [12] for more details). Although one popular method for modular stability analysis is to exploit the passivity formalism and Lyapunov theory, we use contraction theory [12, 24] as an alternative tool for analyzing the modular stability of coupled nonlinear systems. In particular, contraction analysis has more general and intuitive combination properties (e.g., hierarchies) than the passivity method, since it involves a state-space rather than an input-output method. Also, we can straightforwardly prove a stronger form of stability, i.e., globally exponential or globally asymptotic (for a semi-contracting system).

Consider a deterministic and smooth nonlinear system

$$\dot{\mathbf{x}}(t) = \mathbf{f}(\mathbf{x}(t), \mathbf{u}(\mathbf{x}, t), t) \quad (2)$$

where $\mathbf{x}(t) \in \mathcal{R}^n$, and $\mathbf{f} : \mathcal{R}^n \times \mathcal{R}^m \times \mathcal{R}_+ \rightarrow \mathcal{R}^n$. A virtual displacement, $\delta\mathbf{x}$ is defined as an infinitesimal displacement at fixed time — a common supposition in the calculus of variations.

Theorem 1 For the system in (2), if there exists a uniformly positive definite metric,

$$\mathbf{M}(\mathbf{x}, t) = \Theta(\mathbf{x}, t)^T \Theta(\mathbf{x}, t) \quad (3)$$

where Θ is some smooth coordinate transformation of the virtual displacement, $\delta \mathbf{z} = \Theta \delta \mathbf{x}$, such that the associated generalized Jacobian, \mathbf{F} is uniformly negative definite, i.e., $\exists \lambda > 0$ such that

$$\mathbf{F} = \left(\dot{\Theta}(\mathbf{x}, t) + \Theta(\mathbf{x}, t) \frac{\partial \mathbf{f}}{\partial \mathbf{x}} \right) \Theta(\mathbf{x}, t)^{-1} \leq -\lambda \mathbf{I}, \quad (4)$$

then all system trajectories converge globally to a single trajectory exponentially fast regardless of the initial conditions, with a global exponential convergence rate of the largest eigenvalues of the symmetric part of \mathbf{F} .

Such a system is said to be contracting. The proof is given in [12]. Equivalently, the system is contracting if $\exists \lambda > 0$ such that

$$\dot{\mathbf{M}} + \left(\frac{\partial \mathbf{f}}{\partial \mathbf{x}} \right)^T \mathbf{M} + \mathbf{M} \frac{\partial \mathbf{f}}{\partial \mathbf{x}} \leq -2\lambda \mathbf{M} \quad (5)$$

(5) is useful for the stability proof of a Lagrangian system, since the inertia matrix $\mathbf{M}(\mathbf{q})$ of the robot dynamics in (1) can be chosen as the metric \mathbf{M} in (5).

B. Adaptive Synchronization via Active Parameter Estimation

A decentralized adaptive synchronization control law^{4,9,24} that adapts to an unknown, possibly slowly-varying, parametric uncertainties can be designed for a network comprised of p heterogeneous robots ($\mathbf{M}_i \neq \mathbf{M}_j$, $1 \leq i, j \leq p$).

Following [4], let us first consider a network with a two-way-ring symmetric structure. This network structure will be further generalized to realize the full potential of the proposed adaptive strategy in Section IV. The following control law is proposed for the i -th robot ($p \geq 3$):

$$\begin{aligned} \tau_i &= \hat{\mathbf{M}}_i(\mathbf{q}_i) \ddot{\mathbf{q}}_{i,r} + \hat{\mathbf{C}}_i(\mathbf{q}_i, \dot{\mathbf{q}}_i) \dot{\mathbf{q}}_{i,r} + \hat{\mathbf{g}}_i(\mathbf{q}_i) - \mathbf{K}_1(t) \mathbf{s}_i + \mathbf{K}_2(t) \mathbf{s}_{i-1} + \mathbf{K}_2(t) \mathbf{s}_{i+1} \\ &= \mathbf{W}_i \hat{\mathbf{b}}_i - \mathbf{K}_1(t) \mathbf{s}_i + \mathbf{K}_2(t) \mathbf{s}_{i-1} + \mathbf{K}_2(t) \mathbf{s}_{i+1} \end{aligned} \quad (6)$$

where $\mathbf{K}_1(t) \in \mathcal{R}^{n \times n} > 0$ is a tracking control gain matrix, and $\mathbf{K}_2(t) \in \mathcal{R}^{n \times n} > 0$ is a diffusive coupling gain matrix with the adjacent members ($i-1$ and $i+1$). where the common desired time-varying trajectory (or the virtual leader dynamics) is denoted by $\mathbf{q}_d(t)$. The reference velocity vector $\dot{\mathbf{q}}_{i,r}$ is defined as

$$\dot{\mathbf{q}}_{i,r} = \dot{\mathbf{q}}_d - \Lambda \tilde{\mathbf{q}}_i = \dot{\mathbf{q}}_d - \Lambda(\mathbf{q}_i - \mathbf{q}_d) \quad (7)$$

where Λ is a positive diagonal matrix. The composite variable is defined as $\mathbf{s}_i = \dot{\mathbf{q}}_i - \dot{\mathbf{q}}_{i,r}$.

Also, the parameter estimate $\hat{\mathbf{b}}_i$ is the unknown parameters of the i -th robot dynamic model, which is updated by the correlation integral²⁵

$$\dot{\hat{\mathbf{b}}}_i = -\mathbf{\Gamma} \mathbf{W}_i^T \mathbf{s}_i \quad (8)$$

where $\mathbf{\Gamma}$ is a symmetric positive definite matrix. Hence, the closed-loop system for a network comprised of p non-identical robots can be written as

$$\begin{bmatrix} [\mathbf{M}(\mathbf{q})] & \mathbf{0} \\ \mathbf{0} & [\mathbf{\Gamma}^{-1}] \end{bmatrix} \begin{pmatrix} \dot{\mathbf{x}} \\ \dot{\{\tilde{\mathbf{b}}\}} \end{pmatrix} + \begin{bmatrix} [\mathbf{C}(\mathbf{q}, \dot{\mathbf{q}})] & \mathbf{0} \\ \mathbf{0} & \mathbf{0} \end{bmatrix} \begin{pmatrix} \mathbf{x} \\ \{\tilde{\mathbf{b}}\} \end{pmatrix} + \begin{bmatrix} [\mathbf{L}_{\mathbf{K}_1, -\mathbf{K}_2}^p] & -[\mathbf{W}] \\ [\mathbf{W}]^T & \mathbf{0} \end{bmatrix} \begin{pmatrix} \mathbf{x} \\ \{\tilde{\mathbf{b}}\} \end{pmatrix} = \mathbf{0} \quad (9)$$

where $[\mathbf{M}(\mathbf{q})]$ and $[\mathbf{C}(\mathbf{q}, \dot{\mathbf{q}})]$ are the block diagonal matrices of $\mathbf{M}_i(\mathbf{q}_i)$ and $\mathbf{C}_i(\mathbf{q}_i, \dot{\mathbf{q}}_i)$, $i = 1, \dots, p$. The additional block diagonal matrices are defined from (8) such that $[\mathbf{\Gamma}^{-1}] = \text{diag}(\mathbf{\Gamma}^{-1}, \mathbf{\Gamma}^{-1}, \dots, \mathbf{\Gamma}^{-1})_p$, $[\mathbf{W}] = \text{diag}(\mathbf{W}_1, \mathbf{W}_2, \dots, \mathbf{W}_p)$. Also, $\mathbf{x} = (\mathbf{s}_1^T, \mathbf{s}_2^T, \dots, \mathbf{s}_p^T)^T$, and $\{\tilde{\mathbf{b}}\} = (\tilde{\mathbf{b}}_1^T, \tilde{\mathbf{b}}_2^T, \dots, \tilde{\mathbf{b}}_p^T)^T$ where $\tilde{\mathbf{b}}_i$ denotes an error of the parameter estimate such that $\tilde{\mathbf{b}}_i = \tilde{\mathbf{b}}_i - \mathbf{b}_i$. Note that \mathbf{b}_i is a constant vector of the true parameter values for the i -th robot, resulting in $\dot{\tilde{\mathbf{b}}}_i = \dot{\hat{\mathbf{b}}}_i$. If each robot is identical, $\mathbf{b}_i = \mathbf{b}$ for $1 \leq i \leq p$.

$[\mathbf{L}_{\mathbf{K}_1, -\mathbf{K}_2}^p]$ is a modified Laplacian⁴ defined by

$$[\mathbf{L}_{\mathbf{A}, \mathbf{B}}^p] \triangleq \begin{bmatrix} \mathbf{A} & \mathbf{B} & \mathbf{0} & \cdots & \mathbf{B} \\ \mathbf{B} & \mathbf{A} & \mathbf{B} & \cdots & \mathbf{0} \\ \vdots & \vdots & \ddots & \ddots & \vdots \\ \mathbf{0} & \cdots & \mathbf{B} & \mathbf{A} & \mathbf{B} \\ \mathbf{B} & \cdots & \mathbf{0} & \mathbf{B} & \mathbf{A} \end{bmatrix}_{p \times p}. \quad (10)$$

$[\mathbf{U}_{\mathbf{K}_2}^p]$ is a $p \times p$ block square matrix whose elements are \mathbf{K}_2 and it is used in the following theorem.

Theorem 2 *The adaptive synchronization law in (6) globally asymptotically synchronizes the states of multiple dynamics in the presence of parametric model uncertainties if the condition $[\mathbf{L}_{\mathbf{K}_1, -\mathbf{K}_2}^p] + [\mathbf{U}_{\mathbf{K}_2}^p] > 0, \forall t$ holds.*

Proof See [4].

III. Synchronization of Heterogeneous Adaptive Dynamics

A. Synchronization of Adaptive Dynamics using Physical Parameter Adaptation

Assume that the individual robot dynamics of the network are adaptive in the sense that their physical parameters, connoted by \mathbf{a}_i , are now adapting or mutating, according to the adaptation law

$$\dot{\mathbf{a}}_i = \Sigma \mathbf{Y}_i^T \mathbf{s}_i \quad (11)$$

where Σ is a symmetric positive definite matrix. Note that the adaptive parameters are carefully selected such that the inertia matrix $\mathbf{M}_i(\mathbf{q}_i)$ is uniformly positive definite. This is different from (8) where the actual physical parameters of the robot (\mathbf{b}_i) are fixed, but its estimates $\hat{\mathbf{b}}_i$ are updated in the adaptive control law (8). In this section, however, the actual values of \mathbf{a}_i are updated by (11) and the original dynamics in (1) are now called adaptive dynamics. Consider the following control law for the i -th robot

$$\tau_i = \mathbf{Y}_i \mathbf{a}_{\text{leader}} - \mathbf{K}_1 \mathbf{s}_i + \mathbf{K}_2 \mathbf{s}_{i-1} + \mathbf{K}_2 \mathbf{s}_{i+1} \quad (12)$$

where $\mathbf{a}_{\text{leader}}$, which corresponds to the physical parameters of the leader, is slowly varying or constant.

Theorem 3 *The adaptive synchronization law in (12) globally asymptotically synchronizes the states of multiple adaptive dynamics.*

Proof By defining the parametric error $\tilde{\mathbf{a}}_i = \mathbf{a}_i - \mathbf{a}_{\text{leader}}$ and combining (1), (11), and (12), the closed-loop system for a network comprised of p non-identical robots can be written as

$$\begin{bmatrix} [\mathbf{M}(\mathbf{q})] & \mathbf{0} \\ \mathbf{0} & [\Sigma^{-1}] \end{bmatrix} \begin{pmatrix} \dot{\mathbf{x}} \\ \dot{\{\tilde{\mathbf{a}}\}} \end{pmatrix} + \begin{bmatrix} [\mathbf{C}(\mathbf{q}, \dot{\mathbf{q}})] & \mathbf{0} \\ \mathbf{0} & \mathbf{0} \end{bmatrix} \begin{pmatrix} \mathbf{x} \\ \{\tilde{\mathbf{a}}\} \end{pmatrix} + \begin{bmatrix} [\mathbf{L}_{\mathbf{K}_1, -\mathbf{K}_2}^p] [\mathbf{Y}] \\ -[\mathbf{Y}]^T & \mathbf{0} \end{bmatrix} \begin{pmatrix} \mathbf{x} \\ \{\tilde{\mathbf{a}}\} \end{pmatrix} = \mathbf{0} \quad (13)$$

where $[\mathbf{M}(\mathbf{q})]$, $[\mathbf{C}(\mathbf{q}, \dot{\mathbf{q}})]$, and $[\mathbf{Y}]$ are diagonal matrices whose diagonal elements are $\mathbf{M}_i(\mathbf{q}_i)$, $\mathbf{C}_i(\mathbf{q}_i, \dot{\mathbf{q}}_i)$, and \mathbf{Y}_i , respectively. $[\Sigma^{-1}] = \text{diag}(\Sigma^{-1}, \Sigma^{-1}, \dots, \Sigma^{-1})_p$. Moreover, \mathbf{K}_1 and \mathbf{K}_2 are tracking control and diffusive coupling gains such that $\mathbf{K}_1 - 2\mathbf{K}_2 > 0$, $\mathbf{K}_1 > \mathbf{0}$, and $\mathbf{K}_2 > 0$. Note that $[\mathbf{L}_{\mathbf{K}_1, -\mathbf{K}_2}^p]$, a strictly positive definite by the condition of \mathbf{K}_1 and \mathbf{K}_2 , is defined in (10).

Following [4], we can apply the spectral decomposition to (13) by using $\mathbf{V} = [[\mathbf{1}] \quad \mathbf{V}_{\text{sync}}]$, $\mathbf{V}^T [\mathbf{L}_{\mathbf{K}_1, -\mathbf{K}_2}^p] \mathbf{V} = [\mathbf{D}]$ and the augmented $\mathbf{V}_a = \text{diag}(\mathbf{V}, \mathbf{I}_{pn})$. Note that $[\mathbf{1}]$ matrix consists of p identity matrices and that \mathbf{V}_{sync} consists of the orthonormal eigenvectors other than $[\mathbf{1}]$. See [4] for some examples.

This leads to the following virtual system of $(\mathbf{y}_1^T, \mathbf{y}_2^T)^T$ [4, 9, 24]

$$\begin{bmatrix} \mathbf{V}^T [\mathbf{M}(\mathbf{q})] \mathbf{V} & \mathbf{0} \\ \mathbf{0} & [\Sigma^{-1}] \end{bmatrix} \begin{pmatrix} \dot{\mathbf{y}}_1 \\ \dot{\mathbf{y}}_2 \end{pmatrix} + \begin{bmatrix} \mathbf{V}^T [\mathbf{C}(\mathbf{q}, \dot{\mathbf{q}})] \mathbf{V} & \mathbf{0} \\ \mathbf{0} & \mathbf{0} \end{bmatrix} \begin{pmatrix} \mathbf{y}_1 \\ \mathbf{y}_2 \end{pmatrix} + \begin{bmatrix} [\mathbf{D}] & \mathbf{V}^T [\mathbf{Y}] \\ -[\mathbf{Y}]^T \mathbf{V} & \mathbf{0} \end{bmatrix} \begin{pmatrix} \mathbf{y}_1 \\ \mathbf{y}_2 \end{pmatrix} = \mathbf{0}. \quad (14)$$

The virtual system has two particular solutions: $\mathbf{y}_1 = \mathbf{V}^T \mathbf{x}, \mathbf{y}_2 = \{\tilde{\mathbf{a}}\}$, and $\mathbf{y}_1 = \mathbf{0}, \mathbf{y}_2 = \mathbf{0}$. The virtual length analysis indicates that (14) is semi-contracting by the negative semi-definite Jacobian with $[\mathbf{D}] > 0$:

$$\frac{dV}{dt} = -2 \begin{pmatrix} \delta \mathbf{y}_1 \\ \delta \mathbf{y}_2 \end{pmatrix}^T \begin{bmatrix} [\mathbf{D}] & \mathbf{0} \\ \mathbf{0} & \mathbf{0} \end{bmatrix} \begin{pmatrix} \delta \mathbf{y}_1 \\ \delta \mathbf{y}_2 \end{pmatrix} \quad (15)$$

where $V \triangleq \begin{pmatrix} \delta \mathbf{y}_1 \\ \delta \mathbf{y}_2 \end{pmatrix}^T \begin{bmatrix} \mathbf{V}^T [\mathbf{M}(\mathbf{q})] \mathbf{V} & \mathbf{0} \\ \mathbf{0} & [\boldsymbol{\Sigma}^{-1}] \end{bmatrix} \begin{pmatrix} \delta \mathbf{y}_1 \\ \delta \mathbf{y}_2 \end{pmatrix}$ is the virtual length used.

Using Barbalat's lemma, it can be shown that $\delta \mathbf{y}_1$ tends asymptotically to zero from any initial condition. Also, $[\mathbf{D}]$ can be decomposed to the tracking and synchronization gains. Consequently, we can conclude that the states of multiple adaptive dynamics are synchronized by the knowledge feedback from the leader ($\mathbf{Y}_i \mathbf{a}_{\text{leader}}$).

While the synchronization of the physical parameters to the leader is not automatically guaranteed due to the semi-contracting stability of (14), the additional condition of persistency of excitation²⁵ would lead to the convergence of \mathbf{a}_i to $\mathbf{a}_{\text{leader}}$.

Corollary 1 *The convergence rate of $\tilde{\mathbf{a}}_i \rightarrow \mathbf{0}$ can be improved by adding the diffusive coupling of the physical parameters to the adaptation law in (11):*

$$\dot{\mathbf{a}}_i = \boldsymbol{\Sigma} \mathbf{Y}_i^T \mathbf{s}_i - \boldsymbol{\Sigma} \mathbf{P} (\mathbf{a}_i - \mathbf{a}_{\text{leader}}) \quad (16)$$

where \mathbf{P} is positive definite.

Proof It is straightforward to derive the virtual length analysis

$$\frac{dV}{dt} = -2 \begin{pmatrix} \delta \mathbf{y}_1 \\ \delta \mathbf{y}_2 \end{pmatrix}^T \begin{bmatrix} [\mathbf{D}] & \mathbf{0} \\ \mathbf{0} & [\mathbf{P}] \end{bmatrix} \begin{pmatrix} \delta \mathbf{y}_1 \\ \delta \mathbf{y}_2 \end{pmatrix}, \quad (17)$$

which guarantees the globally exponential stability of the multiple adaptive dynamics.

Remark 1 (12) is particularly attractive since it does not need knowledge of its time-varying parameter \mathbf{a}_i . If we regard $\mathbf{q}_d(t)$ of the composite variable \mathbf{s}_i in (12) as the power leader dynamics, this is the case when the knowledge leader and the power leader co-exist.³¹

B. Optimality of the Adaptive Control Based on the Parameter Adaptation

The aim of this section is to show its optimality. This optimality can be checked by using the inverse optimal control problem.^{10,13}

Theorem 4 *The adaptation law in (12) for the closed-loop system for a network comprised of p non-identical robots in (13) minimizes the cost functional J_a*

$$J_a = \int_0^\infty (l(\mathbf{x}, \mathbf{a}) + \mathbf{u}^T \mathbf{R}(\mathbf{x}, \mathbf{a}) \mathbf{u}) dt \quad (18)$$

where

$$l(\mathbf{x}, \mathbf{a}) = -2\beta \left[\frac{\partial V}{\partial \mathbf{x}} \mathbf{f} + \frac{\partial V}{\partial \mathbf{x}} \mathbf{F} \left(\mathbf{a} + \Gamma \left(\frac{\partial V}{\partial \mathbf{a}} \right)^T \right) - \frac{\partial V}{\partial \mathbf{x}} \mathbf{g} \mathbf{R}^{-1} \left(\frac{\partial V}{\partial \mathbf{x}} \mathbf{g} \right)^T \right] + \beta(\beta - 2) \frac{\partial V}{\partial \mathbf{x}} \mathbf{g} \mathbf{R}^{-1} \left(\frac{\partial V}{\partial \mathbf{x}} \mathbf{g} \right)^T$$

where the mappings $\mathbf{f}(\mathbf{x})$, $\mathbf{F}(\mathbf{x})$, and $\mathbf{g}(\mathbf{x})$, defined in (20), are smooth. Moreover, $\Gamma \in \mathcal{R}^{np \times np}$ and $\mathbf{R}(\mathbf{x}, \mathbf{a}) \in \mathcal{R}^{np \times np}$ are symmetric positive definite matrices and $\beta \geq 2$ is constant.

Proof From the first equation in (13), the closed-loop system for a network comprised of p non-identical robots can be written as

$$[\mathbf{M}(\mathbf{q})] \dot{\mathbf{x}} + [\mathbf{C}(\mathbf{q}, \dot{\mathbf{q}})] \mathbf{x} + [\mathbf{Y}] \{\tilde{\mathbf{a}}\} + [\mathbf{L}_{\mathbf{K}_1, -\mathbf{K}_2}^p] \mathbf{x} = \mathbf{0} \quad (19)$$

where $\mathbf{x} = [\mathbf{s}_1 \ \mathbf{s}_2 \ \cdots \ \mathbf{s}_p]^T$ and $\mathbf{s}_i = \dot{\mathbf{q}}_i - \dot{\mathbf{q}}_{ir} = \dot{\mathbf{q}}_i - \dot{\mathbf{q}}_d + \Lambda(\mathbf{q}_i - \mathbf{q}_d)$. Suppose that $[\mathbf{M}(\mathbf{q})]$, $[\mathbf{C}(\mathbf{q}, \dot{\mathbf{q}})]$, and $[\mathbf{Y}]$ are smooth. Then by multiplying both sides of (19) by $[\mathbf{M}(\mathbf{q})]^{-1}$, the nonlinear equation can be rewritten as follows:

$$\dot{\mathbf{x}} = -[\mathbf{M}(\mathbf{q})]^{-1}[\mathbf{C}(\mathbf{q}, \dot{\mathbf{q}})]\mathbf{x} - [\mathbf{M}(\mathbf{q})]^{-1}[\mathbf{Y}]\{\hat{\mathbf{a}}\} - [\mathbf{M}(\mathbf{q})]^{-1}[\mathbf{L}_{\mathbf{K}_1, -\mathbf{K}_2}^p]\mathbf{x}. \quad (20)$$

Therefore, let us define $\mathbf{f}(\mathbf{x})$, $\mathbf{F}(\mathbf{x})$, $\mathbf{g}(\mathbf{x})$, and \mathbf{u} as

$$\begin{aligned} \mathbf{f}(\mathbf{x}) &= -[\mathbf{M}(\mathbf{q})]^{-1}[\mathbf{C}(\mathbf{q}, \dot{\mathbf{q}})] \\ \mathbf{F}(\mathbf{x}) &= -[\mathbf{M}(\mathbf{q})]^{-1}[\mathbf{Y}] \\ \mathbf{g}(\mathbf{x}) &= [\mathbf{M}(\mathbf{q})]^{-1} \\ \mathbf{u} &= -[\mathbf{L}_{\mathbf{K}_1, -\mathbf{K}_2}^p]\mathbf{x}. \end{aligned}$$

If we define the adaptive control Lyapunov function V in [10] as $V(\mathbf{x}, \mathbf{a}, \cdot) = \frac{1}{2}\mathbf{x}^T\mathbf{x} + V_r(\mathbf{a}, \cdot)$, from the condition for optimality characteristics in [10], the following condition should be satisfied:

$$\mathbf{R}(\mathbf{x}, \mathbf{a})^{-1}\mathbf{g}^T = [\mathbf{L}_{\mathbf{K}_1, -\mathbf{K}_2}^p] \quad (21)$$

where \mathbf{g} and $[\mathbf{L}_{\mathbf{K}_1, -\mathbf{K}_2}^p]$ are known. Therefore, if we choose $\mathbf{R}(\mathbf{x}, \mathbf{a})$ such that (21) is satisfied, the proposed adaptive controller for the network system has the optimal characteristics by the results in [10].

C. Potential Applications of Adaptive Synchronization

The benefit of adaptive synchronization is obvious in the case of indifferent tracking,⁵ i.e., $\mathbf{K}_1 = 2\mathbf{K}_2$ in the adaptive control law in (12). Since $\mathbf{V}_{sync}^T\mathbf{x}$ is not a flow-invariant manifold for a heterogeneous network, the heterogeneous dynamics do not synchronize in the absence of exponential tracking stability. Consequently, the knowledge coupling introduced in this section provides a method of both the state and parameter synchronization of heterogeneous adaptive dynamics. Examples of adaptive dynamics include autonomous docking of highly fractionated spacecraft or space robots. In another example, the physical parameters which vary adaptively could also be the local control terms, such as impedance control gains.²⁶ For instance, a group of robot manipulators can share the load of some big object, and actively tune the impedance control gains once some external force is applied to the robot network. The synchronization of the local impedance control gains can also be interpreted in the context of impedance matching of bilateral time-delayed telemanipulation.¹⁷

IV. Proposed Parameter Adaptation for Synchronization

By incorporating the new results from Section III, we present the main adaptive synchronization control law in this section. Although we suggest new parameter adaptation in the previous section, it is difficult to change the physical parameters unless we combine or divide the robots. Accordingly, non-physical parameters such as tracking control and diffusive coupling gains could be good parameters for adaptation. However, changing gains would modify the Laplacian matrix thereby affecting the stability of the network. The main contribution of the section is to introduce the flexibility of the Laplacian matrix without sacrificing the stability and optimality condition of the cooperative control of robotic networks. Moreover, the proposed adaptive cooperative control can be applied to any network structure including two-way-ring and all-to-all structures.

A. Synchronization of Adaptive Dynamics using Parameter Adaptation in Tracking Control and Diffusive Coupling Gains

In this section, the active parameter adaptation is applied to tuning the tracking control gains $\mathbf{K}_{ii}(t)$ and diffusive coupling gains $\mathbf{K}_{il}(t)$ ($i \neq l$). Moreover, the two-way-ring symmetric structure becomes more generalized. For this purpose, by using (6), the proposed adaptive synchronization law can be written as:

$$\begin{aligned} \tau_i &= \mathbf{M}_i(\mathbf{q}_i)\ddot{\mathbf{q}}_{i,r} + \mathbf{C}_i(\mathbf{q}_i, \dot{\mathbf{q}}_i)\dot{\mathbf{q}}_{i,r} + \mathbf{g}_i(\mathbf{q}_i) - \mathbf{K}_{ii}\mathbf{s}_i + \sum_{l=1, l \neq i}^p \mathbf{K}_{il}\mathbf{s}_l \\ &= \mathbf{M}_i(\mathbf{q}_i)\ddot{\mathbf{q}}_{i,r} + \mathbf{C}_i(\mathbf{q}_i, \dot{\mathbf{q}}_i)\dot{\mathbf{q}}_{i,r} + \mathbf{g}_i(\mathbf{q}_i) - \mathbf{T}_i(\mathbf{s})\mathbf{c}_i \\ &= \mathbf{M}_i(\mathbf{q}_i)\ddot{\mathbf{q}}_{i,r} + \mathbf{C}_i(\mathbf{q}_i, \dot{\mathbf{q}}_i)\dot{\mathbf{q}}_{i,r} + \mathbf{g}_i(\mathbf{q}_i) - \mathbf{T}_i(\mathbf{s})\mathbf{c}_i'' - \mathbf{T}_i(\mathbf{s})\mathbf{c}_i' \end{aligned} \quad (22)$$

where $\mathbf{T}_i(\mathbf{s}) = [-\mathbf{s}_1 \ \cdots \ -\mathbf{s}_{i-1} \ +\mathbf{s}_i \ -\mathbf{s}_{i+1} \ \cdots \ -\mathbf{s}_p]$ denotes a $n \times p$ matrix for composite variables of the robotic network and $\mathbf{c}_i = [\mathbf{K}_{i1} \ \mathbf{K}_{i2} \ \cdots \ \mathbf{K}_{ip}]^T$ denotes a vector for control gain such that $\mathbf{c}_i = \mathbf{c}_i'' + \mathbf{c}_i'$, respectively. \mathbf{K}_{il} denotes the control gains of the i -th robot for tracking control (for $l = i$) as well as diffusive coupling with the l -th robot (for $l \neq i$). $\mathbf{c}_i'' = [\mathbf{K}_{i1}'' \ \mathbf{K}_{i2}'' \ \cdots \ \mathbf{K}_{ii-1}'' \ \mathbf{K}_{ii}'' \ \mathbf{K}_{ii+1}'' \ \cdots \ \mathbf{K}_{ip}'']^T$ must follow the conditions that every row sums for p systems be same and the matrix consisting of p row vectors (\mathbf{c}_i'') be symmetric. The matrix satisfying these two conditions is the modified Laplacian,⁴ which describes the two-way ring structure in the p robotic networks. Therefore, we can define $\mathbf{c}_i'' = [\mathbf{0} \ \mathbf{0} \ \cdots \ -\mathbf{K}_2'' \ \mathbf{K}_1'' \ -\mathbf{K}_2'' \ \cdots \ \mathbf{0}]^T$ such that $\mathbf{K}_1'' - 2\mathbf{K}_2'' > \mathbf{0}$, $\mathbf{K}_1'' > \mathbf{0}$, and $\mathbf{K}_2'' > \mathbf{0}$. $\mathbf{c}_i' = [\mathbf{K}'_{i1} \ \mathbf{K}'_{i2} \ \cdots \ \mathbf{K}'_{ip}]$ is a vector whose elements are control gains of the i -th robot and the elements are tuned automatically by using the adaptation law described below. That is, the individual robot dynamics of the network are adaptive in the sense that their tracking control and diffusive coupling gains, connoted by \mathbf{c}_i' , are now adapting according to the adaptation law

$$\dot{\mathbf{c}}_i' = \mathbf{\Sigma}_i \mathbf{T}_i^T(\mathbf{s}_i) \mathbf{s}_i \quad (23)$$

where $\mathbf{\Sigma}_i$ is a symmetric positive definite matrix and $\mathbf{\Sigma}_i = \text{diag}(\sigma_1, \sigma_2, \dots, \sigma_p)$ such that $\sigma_1 = \sigma_2 = \dots = \sigma_{i-1} = \sigma_{i+1} = \dots = \sigma_p$. That is, only σ_i has a different value in $\mathbf{\Sigma}_i$.

This is similar to (11) in the sense that these two adaptation laws update parameters of the robot dynamics. However, updated parameters in (23) are tracking control and diffusive coupling gains while those in (11) are physical parameters such as mass, volumes, etc.

Theorem 5 *The adaptive synchronization law in (22) globally asymptotically synchronizes the states of multiple adaptive dynamics.*

Proof From (1) and (22), the closed-loop dynamics for the i -th robot can be expressed as

$$\mathbf{M}_i(\mathbf{q}_i) \dot{\mathbf{s}}_i + \mathbf{C}_i(\mathbf{q}_i, \dot{\mathbf{q}}_i) \mathbf{s}_i + \mathbf{T}_i(\mathbf{s}) \mathbf{c}_i' + \mathbf{K}_1'' \mathbf{s}_i - \mathbf{K}_2'' \mathbf{s}_{i-1} - \mathbf{K}_2'' \mathbf{s}_{i+1} = \mathbf{0}. \quad (24)$$

where the fixed gains \mathbf{K}_1'' and \mathbf{K}_2'' are chosen such that $\mathbf{K}_1'' - 2\mathbf{K}_2'' > \mathbf{0}$, $\mathbf{K}_1'' > \mathbf{0}$, and $\mathbf{K}_2'' > \mathbf{0}$.

This system follows the adaptation law described in (23). The closed-loop system for a network and the parameter adaptation law comprised of p adaptive robot systems can be written as

$$\begin{aligned} [\mathbf{M}(\mathbf{q})] \dot{\mathbf{x}} + [\mathbf{C}(\mathbf{q}, \dot{\mathbf{q}})] \mathbf{x} + [\mathbf{L}_{\mathbf{K}_1'', -\mathbf{K}_2''}^p] \mathbf{x} + [\mathbf{T}(\mathbf{s})] \{\mathbf{c}'\} &= \mathbf{0} \\ \{\dot{\mathbf{c}}'\} &= [\mathbf{\Sigma}] [\mathbf{T}(\mathbf{s})]^T \mathbf{x} \end{aligned}$$

or by combining these two equations, it can be expressed as follows:

$$\begin{bmatrix} [\mathbf{M}(\mathbf{q})] & \mathbf{0} \\ \mathbf{0} & [\mathbf{\Sigma}^{-1}] \end{bmatrix} \begin{pmatrix} \dot{\mathbf{x}} \\ \{\dot{\mathbf{c}}'\} \end{pmatrix} + \begin{bmatrix} [\mathbf{C}(\mathbf{q}, \dot{\mathbf{q}})] & \mathbf{0} \\ \mathbf{0} & \mathbf{0} \end{bmatrix} \begin{pmatrix} \mathbf{x} \\ \{\mathbf{c}'\} \end{pmatrix} + \begin{bmatrix} [\mathbf{L}_{\mathbf{K}_1'', -\mathbf{K}_2''}^p] & [\mathbf{T}(\mathbf{s})] \\ -[\mathbf{T}(\mathbf{s})]^T & \mathbf{0} \end{bmatrix} \begin{pmatrix} \mathbf{x} \\ \{\mathbf{c}'\} \end{pmatrix} = \mathbf{0} \quad (25)$$

where $[\mathbf{\Sigma}^{-1}] = \text{diag}(\mathbf{\Sigma}_1^{-1}, \mathbf{\Sigma}_2^{-1}, \dots, \mathbf{\Sigma}_p^{-1})$. Moreover, $[\mathbf{L}_{\mathbf{K}_1'', -\mathbf{K}_2''}^p]$ is a symmetric positive definite by the condition of \mathbf{K}_1'' and \mathbf{K}_2'' , which is a modified Laplacian, defined in (10). For example, a two-way ring structure has

$$[\mathbf{L}_{\mathbf{K}_1'', -\mathbf{K}_2''}^p] \triangleq \begin{bmatrix} \mathbf{K}_1'' & -\mathbf{K}_2'' & \mathbf{0} & \cdots & -\mathbf{K}_2'' \\ -\mathbf{K}_2'' & \mathbf{K}_1'' & -\mathbf{K}_2'' & \cdots & \mathbf{0} \\ \vdots & \vdots & \vdots & \ddots & \vdots \\ -\mathbf{K}_2'' & \cdots & \mathbf{0} & -\mathbf{K}_2'' & \mathbf{K}_1'' \end{bmatrix}_{p \times p}.$$

Similar to Theorem 3, by applying the spectral transformation, using the augmented $\mathbf{V}_a = \text{diag}(\mathbf{V}, \mathbf{I}_{pn})$ and $\mathbf{V}^T [\mathbf{L}_{\mathbf{K}_1'', -\mathbf{K}_2''}^p] \mathbf{V} = [\mathbf{D}']$, to (25) leads to the following virtual system of $(\mathbf{y}_1^T, \mathbf{y}_2^T)^T$

$$\begin{bmatrix} \mathbf{V}^T [\mathbf{M}(\mathbf{q})] \mathbf{V} & \mathbf{0} \\ \mathbf{0} & [\mathbf{\Sigma}^{-1}] \end{bmatrix} \begin{pmatrix} \dot{\mathbf{y}}_1 \\ \dot{\mathbf{y}}_2 \end{pmatrix} + \begin{bmatrix} \mathbf{V}^T [\mathbf{C}(\mathbf{q}, \dot{\mathbf{q}})] \mathbf{V} & \mathbf{0} \\ \mathbf{0} & \mathbf{0} \end{bmatrix} \begin{pmatrix} \mathbf{y}_1 \\ \mathbf{y}_2 \end{pmatrix} + \begin{bmatrix} [\mathbf{D}'] & \mathbf{V}^T [\mathbf{T}(\mathbf{s})] \\ -[\mathbf{T}(\mathbf{s})]^T \mathbf{V} & \mathbf{0} \end{bmatrix} \begin{pmatrix} \mathbf{y}_1 \\ \mathbf{y}_2 \end{pmatrix} = \mathbf{0}. \quad (26)$$

The virtual system has two particular solutions: $\mathbf{y}_1 = \mathbf{V}^T \mathbf{x}$, $\mathbf{y}_2 = \{\mathbf{c}'\}$, and $\mathbf{y}_1 = \mathbf{0}$, $\mathbf{y}_2 = \mathbf{0}$. The virtual length analysis indicates that (26) is semi-contracting by the negative semi-definite Jacobian with $[\mathbf{D}'] > \mathbf{0}$:

$$\frac{dV}{dt} = -2 \begin{pmatrix} \delta \mathbf{y}_1 \\ \delta \mathbf{y}_2 \end{pmatrix}^T \begin{bmatrix} [\mathbf{D}'] & \mathbf{0} \\ \mathbf{0} & \mathbf{0} \end{bmatrix} \begin{pmatrix} \delta \mathbf{y}_1 \\ \delta \mathbf{y}_2 \end{pmatrix}. \quad (27)$$

Using Barbalat's lemma, it is straightforward to show that $\delta\mathbf{y}_1$ tends asymptotically to zero from any initial condition. Also, $[\mathbf{D}']$ can be decomposed to the tracking and synchronization gains. Consequently, we can conclude that the states of multiple adaptive dynamics are synchronized by the adaptive feedback in local control gains.

Corollary 2 *If the adaptation law (23) is defined by*

$$\dot{\mathbf{c}}'_i = \Sigma_i \mathbf{T}_i^T(\mathbf{s}) \mathbf{s}_i - \Sigma_i \mathbf{P} \mathbf{c}'_i, \quad (28)$$

this adaptation law globally exponentially synchronizes the states of multiple adaptive dynamics.

Proof The closed-loop system for the network comprised of p adaptive robots using the adaptation law (28) can be written as

$$\begin{bmatrix} [\mathbf{M}(\mathbf{q})] & \mathbf{0} \\ \mathbf{0} & [\Sigma^{-1}] \end{bmatrix} \begin{pmatrix} \dot{\mathbf{x}} \\ \{\dot{\mathbf{c}}'\} \end{pmatrix} + \begin{bmatrix} [\mathbf{C}(\mathbf{q}, \dot{\mathbf{q}})] & \mathbf{0} \\ \mathbf{0} & \mathbf{0} \end{bmatrix} \begin{pmatrix} \mathbf{x} \\ \{\mathbf{c}'\} \end{pmatrix} + \begin{bmatrix} [\mathbf{L}_{\mathbf{K}''_1, -\mathbf{K}''_2}^p] [\mathbf{T}(\mathbf{s})] \\ -[\mathbf{T}(\mathbf{s})]^T & [\mathbf{P}] \end{bmatrix} \begin{pmatrix} \mathbf{x} \\ \{\mathbf{c}'\} \end{pmatrix} = \mathbf{0}. \quad (29)$$

It is straightforward to derive the virtual length analysis

$$\frac{dV}{dt} = -2 \begin{pmatrix} \delta\mathbf{y}_1 \\ \delta\mathbf{y}_2 \end{pmatrix}^T \begin{bmatrix} [\mathbf{D}'] & \mathbf{0} \\ \mathbf{0} & [\mathbf{P}] \end{bmatrix} \begin{pmatrix} \delta\mathbf{y}_1 \\ \delta\mathbf{y}_2 \end{pmatrix} \quad (30)$$

where V denotes the virtual length which was defined in (15). Therefore, it guarantees the globally exponential stability of the multiple adaptive dynamics.

Remark 2 (22) is a desirable control law for the synchronization stability of a complex network system since control designers do not need to consider the exact values of the coupling gains depending on a particular graph topology of the network. For example, the tracking control gain (\mathbf{K}'_1) should be larger than the diffusive coupling gain (\mathbf{K}'_2) on a regular network.⁴ The gains (\mathbf{K}'_{il}) are automatically calculated based on both the adaptation law (23), the synchronization, and tracking errors.

Remark 3 If \mathbf{c}'_i is replaced by $\mathbf{c}_{\text{leader}}$ in (22), the control law reduces to the same knowledge feedback control in (12). Moreover, (28) and (16) become equivalent while they guarantee the globally exponential synchronization. Therefore, (22) and (28) are the general expressions for knowledge feedback control. Moreover, the stability proof is simpler and more concise than what is found in [31].

Remark 4 As mentioned in this section, the tracking control and diffusive coupling gains are calculated automatically by the tracking errors, the synchronization errors, and the active synchronization law. Therefore, the overall control gains might have different values by the information. Moreover, even in the homogenous robotic network, the control gains might have different control gains. The important result is that the values are automatically calculated, not by the control system designers.

B. Optimality of the Proposed Adaptive Control

The proposed adaptive control in this section is also based on the knowledge feedback control as those in the previous section. We want to also show the optimality of the proposed adaptive control by means of using Theorem 4. Optimal control is a process of determining control inputs and state trajectories for a dynamic system over a period of time to minimize a cost functional. Therefore, if the proposed adaptive cooperative control has the optimality, the overall control inputs can be determined, so that the parameter adaptation of control gains can have optimum values for minimizing the cost functional.

Theorem 6 *The adaptive control law in (22) for the closed-loop system for a network comprised of p non-identical robots in (13) minimizes the cost functional J_a in (18).*

Proof It is a straightforward extension of the proof in Theorem 4. Therefore, the proof is omitted.

Theorem 6 shows the optimality of the proposed adaptive cooperative control in robotic networks. Therefore, the values of the control gains by the active adaptation law can be guaranteed the optimum of the values. In the next section, we will show the symmetry of the diffusive coupling gains of the proposed adaptive control, so that the systems' computational burden can be reduced.

C. Symmetry of the Diffusive Coupling Gains

We will evaluate the symmetry of the diffusive coupling gains between the corresponding robots (that is, $\mathbf{K}_{ij} = \mathbf{K}_{ji}$) in the proposed adaptive cooperative control is evaluated. By the definition, $\mathbf{K}_{ij}(t) = \mathbf{K}_{ij}'' + \mathbf{K}'_{ij}(t)$ where \mathbf{K}_{ij}'' and $\mathbf{K}'_{ij}(t)$ denote a fixed gain and a time-varying gain obtained by the active adaptation law, respectively. It is assumed that \mathbf{K}_{ij}'' and \mathbf{K}_{ji}'' have the same values from the condition of the modified Laplacian matrix.⁴ Hence, if $\mathbf{K}'_{ij}(t)$ is equal to $\mathbf{K}'_{ji}(t)$, the symmetry of the diffusive coupling gains can be proven.

Let us write the active parameter adaptation law in (23) again

$$\dot{\mathbf{c}}'_i = \boldsymbol{\Sigma}_i \mathbf{T}_i^T(\mathbf{s}_i) \mathbf{s}_i$$

where $\mathbf{c}'_i = [\mathbf{K}'_{i1} \ \mathbf{K}'_{i2} \ \cdots \ \mathbf{K}'_{ip}]$.

The above adaptation law can be written element-wise. That is, the adaptation law for the diffusive coupling gain of the j -th robot with respect to the i -th robot, calculated in the i -th robot can be written as

$$\dot{\mathbf{K}}'_{ji} = \sigma_j \mathbf{s}_j^T \mathbf{s}_i.$$

In the same way, the adaptation law for the diffusive coupling gain of the i -th robot with respect to the j -th robot, calculated in the j -th robot can be written as

$$\dot{\mathbf{K}}'_{ij} = \sigma_i \mathbf{s}_i^T \mathbf{s}_j.$$

Note that $\sigma_i = \sigma_j$ when $i \neq j$ by the definition of $\boldsymbol{\Sigma}_i$ in (23). Moreover, $\mathbf{s}_j^T \mathbf{s}_i = \mathbf{s}_i^T \mathbf{s}_j$. Therefore, the value of $\dot{\mathbf{K}}'_{ji}(t)$ is always the same as that of $\dot{\mathbf{K}}'_{ij}(t)$. If the initial values of the $\mathbf{K}'_{ji}(t)$ and $\mathbf{K}'_{ij}(t)$ are the same, the two gain values will have identical values.

D. Hybrid Adaptive Synchronization

The proposed adaptive synchronization law in (22) is extended to a hybrid form that combines the adaptation laws for both parameter estimation and active gain variation. Hence, we present a more generalized adaptive synchronization law than (22) that is only applicable to the exactly known systems.

For synchronization of a generalized network structure, we employ two different adaptation laws for parameter estimation and gain adaptation as follows:

$$\begin{aligned} \tau_i &= \hat{\mathbf{M}}_i(\mathbf{q}_i) \ddot{\mathbf{q}}_{i,r} + \hat{\mathbf{C}}_i(\mathbf{q}_i, \dot{\mathbf{q}}_i) \dot{\mathbf{q}}_{i,r} + \hat{\mathbf{g}}_i(\mathbf{q}_i) - \mathbf{K}_{ii} \mathbf{s}_i + \sum_{l=1, l \neq i}^p \mathbf{K}_{il} \mathbf{s}_l \\ &= \mathbf{W}_i \hat{\mathbf{b}}_i - \mathbf{T}_i(\mathbf{s}) \mathbf{c}_i = \mathbf{W}_i \hat{\mathbf{b}}_i - \mathbf{T}_i(\mathbf{s}) \mathbf{c}_i'' - \mathbf{T}_i(\mathbf{s}) \mathbf{c}'_i \end{aligned} \quad (31)$$

where $\hat{\mathbf{b}}_i$ and \mathbf{c}_i denote physical parameters and control gains (tracking control and diffusive coupling gains) for the robot dynamics, respectively. Note that \mathbf{c}_i'' is defined in (22) while $\hat{\mathbf{b}}_i$ and \mathbf{c}'_i actively change the values by using (8) and (23), respectively.

Theorem 7 *The hybrid adaptive synchronization law in (31) with the adaptation laws in (8) and (23) globally asymptotically synchronizes the states of multiple adaptive dynamics in the presence of parametric model uncertainties.*

Proof First, from (1) and (31), the closed-loop dynamics with unknown physical parameters for the i -th robot can be described as

$$\mathbf{M}_i(\mathbf{q}_i) \dot{\mathbf{s}}_i + \mathbf{C}_i(\mathbf{q}_i, \dot{\mathbf{q}}_i) \mathbf{s}_i - \mathbf{W}_i \tilde{\mathbf{b}}_i + \mathbf{T}_i(\mathbf{s}) \mathbf{c}'_i + \mathbf{K}_1'' \mathbf{s}_i - \mathbf{K}_2'' \mathbf{s}_{i-1} - \mathbf{K}_2'' \mathbf{s}_{i+1} = \mathbf{0} \quad (32)$$

where $\tilde{\mathbf{b}}_i = \hat{\mathbf{b}}_i - \mathbf{b}_i$ denotes the error of parameter estimates. Moreover, the fixed control gains \mathbf{K}_1'' and \mathbf{K}_2'' are chosen such that $\mathbf{K}_1'' - 2\mathbf{K}_2'' > \mathbf{0}$, $\mathbf{K}_1'' > \mathbf{0}$, and $\mathbf{K}_2'' > \mathbf{0}$.

Then, by combining (32), (8), and (23), the closed-loop system for a network comprised of p non-identical robots having unknown physical parameters can be written as

$$\begin{bmatrix} [\mathbf{M}(\mathbf{q})] & \mathbf{0} & \mathbf{0} \\ \mathbf{0} & [\mathbf{\Gamma}^{-1}] & \mathbf{0} \\ \mathbf{0} & \mathbf{0} & [\mathbf{\Sigma}^{-1}] \end{bmatrix} \begin{pmatrix} \dot{\mathbf{x}} \\ \{\dot{\tilde{\mathbf{b}}}\} \\ \{\dot{\mathbf{c}}'\} \end{pmatrix} + \begin{bmatrix} [\mathbf{C}(\mathbf{q}, \dot{\mathbf{q}})] & \mathbf{0} & \mathbf{0} \\ \mathbf{0} & \mathbf{0} & \mathbf{0} \\ \mathbf{0} & \mathbf{0} & \mathbf{0} \end{bmatrix} \begin{pmatrix} \mathbf{x} \\ \{\tilde{\mathbf{b}}\} \\ \{\mathbf{c}'\} \end{pmatrix} + \begin{bmatrix} [\mathbf{L}_{\mathbf{K}_1'', -\mathbf{K}_2''}^p] - [\mathbf{W}] [\mathbf{T}(\mathbf{s})] \\ [\mathbf{W}]^T & \mathbf{0} & \mathbf{0} \\ -[\mathbf{T}(\mathbf{s})]^T & \mathbf{0} & \mathbf{0} \end{bmatrix} \begin{pmatrix} \mathbf{x} \\ \{\tilde{\mathbf{b}}\} \\ \{\mathbf{c}'\} \end{pmatrix} = \mathbf{0} \quad (33)$$

where $[\mathbf{L}_{\mathbf{K}_1'', -\mathbf{K}_2''}^p]$ is a symmetric positive definite by the condition of \mathbf{K}_1'' and \mathbf{K}_2'' , which is defined in (25). It is straightforward to show that the synchronization law globally asymptotically synchronizes the states of the multiple adaptive dynamics by using Theorem 3. The remainder of the proof can be derived from Theorem 3.

V. Numerical Validation

We evaluate the superiority reliability of the proposed adaptive cooperative control presented in the previous sections. Two different models are used; one is the linear mass-spring-damper cart system, which can be regarded as a simple robotic network, the other is a highly coupled spacecraft formation flying system. Both systems have heterogeneous agents.

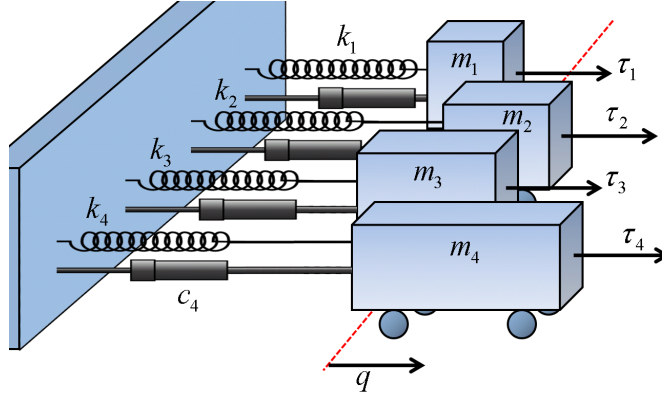


Figure 2. Mass-spring-damper cart system for synchronization of linear heterogeneous robotic network.

A. Linear Mass-Spring-Damper Cart System

It is assumed that there are four carts each of which consists of a mass, a spring, and a damper (Figure 2). We want to synchronize the positions (q_i , $i = 1, 2, 3, 4$) of the carts by using forces τ_i , $i = 1, 2, 3, 4$. It is supposed that the values of masses, springs, and dampers are not same for each cart (that is, the systems is heterogeneous.), but they are constant (that is, the system can be described as a linear second order different equation.). It is further assumed that all carts can measure the exact values of the state values of the other carts as well as those of themselves.

For simulation, all constants are set as follows: masses of the carts are $m_1 = 5$ kg, $m_2 = 2m_1$, $m_3 = 3m_1$, $m_4 = 4m_1$, damping coefficients are $c_1 = 0.04$, $c_2 = 0.03$, $c_3 = 0.02$, $c_4 = 0.01$, and spring constants are $k_1 = k_2 = k_3 = k_4 = 10$, respectively. The desired motion (q_d) is set to $q_d(t) = \sin(2\pi \times 0.1t)$. The initial positions of the carts are assumed to be $q_1(0) = 0.5$ m, $q_2(0) = 1.0$ m, $q_3(0) = -0.5$ m, and $q_4(0) = -1.0$ m, respectively. We assume that the tracking control and diffusive coupling gains are not properly chosen, so that the values are set to $K_1'' = 3$ and $K_2'' = 1$, which will show the superiority of the proposed adaptive cooperative control even in the condition that the system does not have well defined control gains.

Figure 3 shows the state trajectories of the carts by the proposed adaptive control approach and the constant control approach with three different gain selections: minimum, average, and maximum gains,

respectively. The gains are defined as follows:

$$\begin{aligned} \text{Minimum gain : } K_{1,const} &= K_{1,adapt}(0) = K_1'' + K_1'(0) \\ \text{Average gain : } K_{1,const} &= \frac{1}{4} \sum_{i=1}^4 K_{ii,adapt}(t) = \frac{1}{4} \sum_{i=1}^4 (K_{ii,adapt}'' + K_{ii,adapt}') \\ \text{Maximum gain : } K_{1,const} &= \max(K_{ii,adapt}(t)), \quad i = 1, 2, 3, 4. \end{aligned}$$

The diffusive coupling gains for constant cooperative control ($K_{2,const}$) is calculated by $K_{2,const} = \frac{1}{3}K_{1,const}$.

Since two approaches guarantee the globally asymptotic stability for the synchronization, the errors of both the absolute and the relative position converge asymptotically. The proposed adaptive control approach actively adapts the control gains (Figure 4) by using state errors, relative errors, and active synchronization law, so that the errors effectively converge asymptotically, while the constant control approach with the minimum gains takes much more time and needs more control inputs (momentum changes) to reduce errors to acceptable boundary (Table 1). Constant controls with the average and the maximum gains can reduce the convergent time similar to that of the proposed adaptive control approach, while the amount of control inputs cannot be reduced simultaneously.

Note that each diffusive control gain corresponding two carts (that is, $K_{ij} = K_{ji}, i \neq j$) in the proposed adaptive cooperative control approach have the same values (Figure 4). We described the reason in the previous section. Therefore, the computational burden for the whole system can be reduced by sharing the computation for the diffusive coupling gains. Moreover we could expect the reliability of the proposed adaptive cooperative control in the linear cooperative control system even with improperly defined control gains. In the next part, we will evaluate the proposed adaptive control with highly coupled spacecraft formation flying system. The hybrid adaptive cooperative control is also evaluated.

B. Nonlinear Heterogeneous Spacecraft Formation Flying

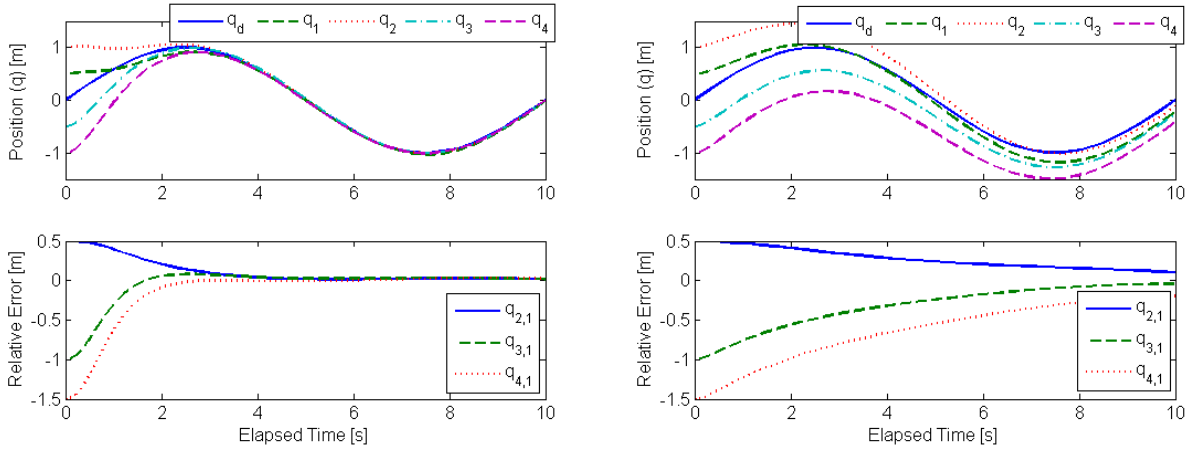
As a robotic network, attitude control for synchronization of the heterogeneous spacecraft formation flying system is a good example, which has highly nonlinear dynamic models.^{2,5} Performance of the proposed adaptive cooperative control law is compared with three cooperative control laws which use constant tracking and diffusive coupling gains. Moreover, the optimality of the proposed adaptive control is evaluated. Consider the formation network that consists of six heterogeneous spacecraft, whose attitudes are described by Modified Rodrigues parameters (MRPs). It is assumed that there is no constraint in actuator. The moments of inertia (MOI) for the four spacecraft are set as follows:

$$\mathbf{J}_1 = \begin{bmatrix} 30 & 0 & -10 \\ 0 & 50 & 0 \\ -10 & 0 & 60 \end{bmatrix}, \quad \mathbf{J}_2 = 2\mathbf{J}_1, \quad \mathbf{J}_3 = 3\mathbf{J}_1, \quad \mathbf{J}_4 = 4\mathbf{J}_1, \quad \mathbf{J}_5 = 5\mathbf{J}_1, \quad \text{and} \quad \mathbf{J}_6 = 6\mathbf{J}_1.$$

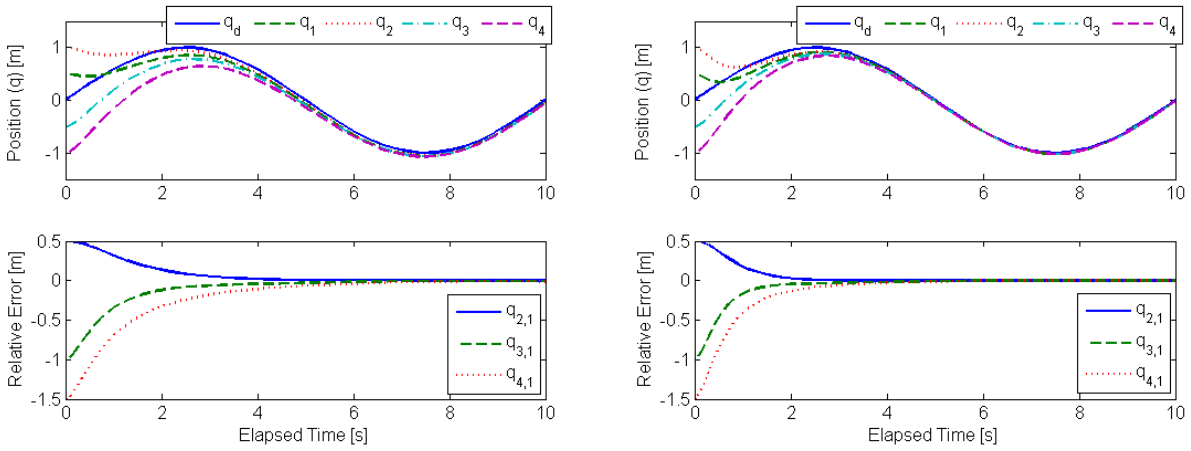
The desired trajectory for the MRPs are $q_{1d}(t) = 0.3 \sin(2\pi \times 0.005t)$, $q_{2d}(t) = 0.2 \sin(2\pi \times 0.01t + \pi/6)$, and $q_{3d}(t) = 0$, respectively. In order to compare the results with those of the constant cooperative controls, the system is assumed to be of a two-way-ring symmetric structure. Note that the proposed adaptive cooperative control can be applied to any network structure. The symmetric positive definite matrix for the parameter adaptation matrix is set to $\Sigma_1 = \text{diag}(10, 5, 0, 0, 5, 5)$, $\Sigma_2 = \text{diag}(5, 10, 5, 0, 0, 0)$, $\Sigma_3 = \text{diag}(0, 0, 0, 5, 10, 5)$, and $\Sigma_4 = \text{diag}(5, 0, 0, 0, 5, 10)$, respectively. The constant Λ , used in the composite variables (\mathbf{s}_i), is set to $\Lambda = 7$. Initial values of the MRPs for the six spacecraft are $\mathbf{q}_1(0) = [0.2, -0.2, 0.1]^T$ rad, $\mathbf{q}_2(0) = [-0.3, 0.0, 0.2]^T$ rad, $\mathbf{q}_3(0) = [0.2, 0.2, -0.2]^T$ rad, $\mathbf{q}_4(0) = [0.1, 0.3, -0.1]^T$ rad, $\mathbf{q}_5(0) = [0.1, 0.2, -0.1]^T$ rad, and $\mathbf{q}_6(0) = [-0.3, 0.1, -0.1]^T$ rad, respectively.

1. Simulation I: Performance of the Proposed Adaptive Cooperative Control

The aim of this simulation is to show the performance of the proposed adaptive cooperative control. Three different constant cooperative controls are used (minimum, average, and maximum gains) for comparison, which were defined in the previous numerical validation. For the proposed adaptive cooperative control, $\mathbf{K}_1'' = 60\mathbf{I}_3$, $\mathbf{K}_2'' = 20\mathbf{I}_3$ are used for the fixed part (where \mathbf{I}_3 is a 3×3 identity matrix) and the values of \mathbf{K}_{il}' ($i = 1, 2, 3, 4, 5, 6$, $l = 1, 2, 3, 4, 5, 6$) are calculated by the active synchronization law. The initial



(a) proposed adaptive control with $K_1'' = 3.0$ and $K_2'' = 1.0$ (b) constant control with minimum control gains ($K_1 = 3.0$ and $K_2 = 1.0$)



(c) constant control with average control gains ($K_1 = 12.2348$ and $K_2 = 4.0783$) (d) constant control with maximum control gains ($K_1 = 23.2757$ and $K_2 = 7.7586$)

Figure 3. State trajectories and relative errors with respect to q_1 by the proposed adaptive control and the constant control with three different control gains. The gains are chosen by the adaptive control gain information.

Table 1. Convergent time (t at $|q| \leq 0.05$ m, $\forall q$) and total momentum changes by the adaptive control and the constant controls with three different conditions (minimum ($K_1 = 3.0$, $K_2 = 1.0$), average ($K_1 = 12.2348$ and $K_2 = 4.0783$), and maximum values ($K_1 = 23.2757$ and $K_2 = 7.7586$))

	Adaptive control	Constant control		
		Minimum gain	Average gain	Maximum gain
Convergent time [s]	3.35	80.22	10.39	3.97
Momentum [Ns]	15.43	120.22	24.72	23.23

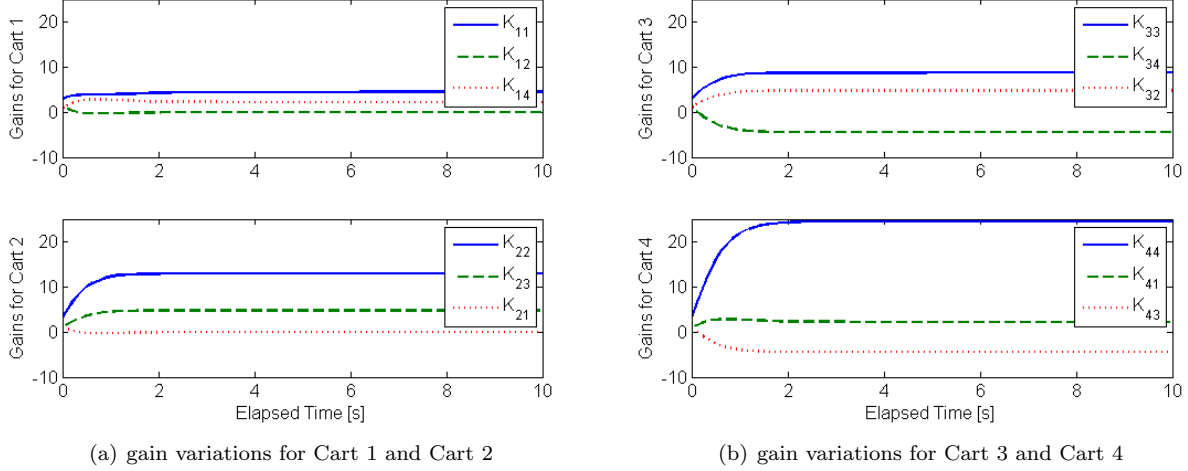


Figure 4. Time histories of the control gain variations by the proposed adaptive control for the linear mass-spring-damper cart system

conditions for \mathbf{K}'_{il} ($i = 1, 2, 3, 4, 5, 6$, $l = 1, 2, 3, 4, 5, 6$) are set to $\mathbf{K}'_{il}(0) = 0$. For the constant cooperative controls, $\mathbf{K}_1 = 60\mathbf{I}_3$ and $\mathbf{K}_2 = 20\mathbf{I}_3$ are used for the minimum gain control, $\mathbf{K}_1 = 237.7240\mathbf{I}_3$ and $\mathbf{K}_2 = 79.2413\mathbf{I}_3$ are used for the average gain control, and $\mathbf{K}_1 = 278.7420\mathbf{I}_3$ and $\mathbf{K}_2 = 92.9140\mathbf{I}_3$ are used for the maximum gain control, respectively. The system is assumed to be of a two-way-ring symmetric structure.

Figure 5 shows the state trajectories by the proposed adaptive cooperative control and three different constant cooperative controls. From the figures (b), (c), and (d), as the control gains are increased, the state trajectories become similar to those of the proposed adaptive control approach (figure (a)), while the control inputs (total angular momentum changes) are increased (Table 2). In the proposed adaptive cooperative control case, however, the convergent time is shorter while control input is less than those of the constant control approaches.

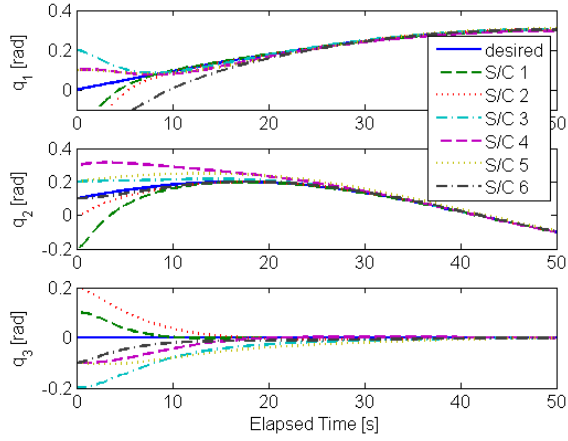
Figures 6 and 7 show the time histories of all control gains in the proposed adaptive cooperative control and the final results for the topology by the proposed adaptive cooperative control and the three different constant cooperative controls. The gain values in the proposed adaptive cooperative control are automatically obtained from the active synchronization law. It should be noted that not all values are positive (e.g., \mathbf{K}_{12} and \mathbf{K}_{34}). That is, the optimized gain values shows that some positive diffusive coupling gains can hinder the efficient convergence of the system. Therefore, the proposed adaptive cooperative control is much superior than the constant cooperative control in a highly nonlinear heterogeneous robotic network.

Table 2. Convergent time (t at $|\mathbf{q}| \leq 0.001 \text{ rad}, \forall \mathbf{q}$) and total angular momentum changes by the proposed adaptive control and the constant controls with three different conditions (minimum ($\mathbf{K}_1 = 60.0$, $\mathbf{K}_2 = 20.0$), average ($\mathbf{K}_1 = 237.7240$ and $\mathbf{K}_2 = 79.2413$), and maximum values ($\mathbf{K}_1 = 278.7420$ and $\mathbf{K}_2 = 92.9140$)) for the spacecraft formation flying system

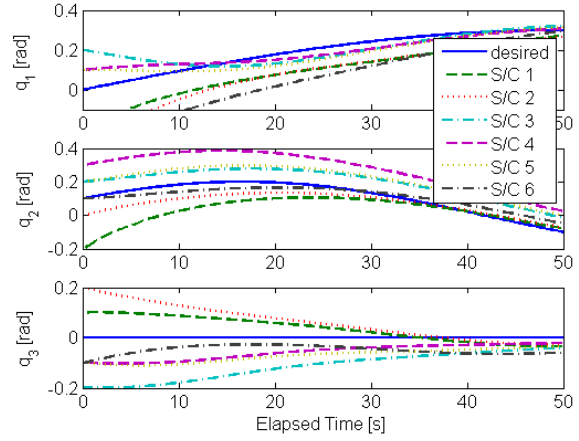
	Adaptive control	Constant control		
		Minimum gain	Average gain	Maximum gain
Convergent time [s]	86.84	521.21	130.02	119.29
Angular momentum [Nms]	32.62	42.17	49.54	54.60

2. Simulation II: Performance of the Proposed Hybrid Adaptive Cooperative Control

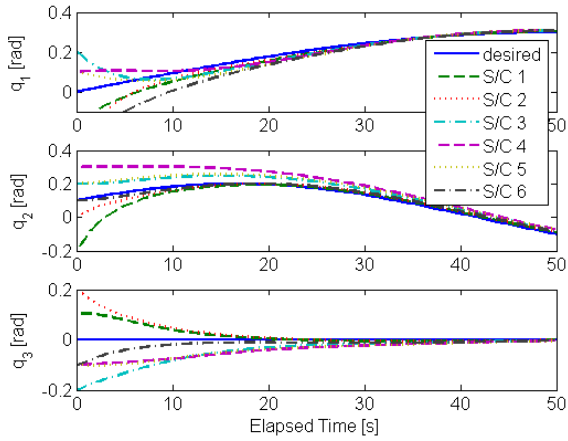
In this simulation, we will evaluate the reliability of the proposed hybrid adaptive cooperative control, mentioned in Section IV.D. The constant cooperative control, used here for comparison, is similar to that used in [4]. For simulation, it is assumed that we do not know the values of the moments of the all spacecraft. For simplicity, first four spacecraft are used for simulation. The real values of the MOIs are



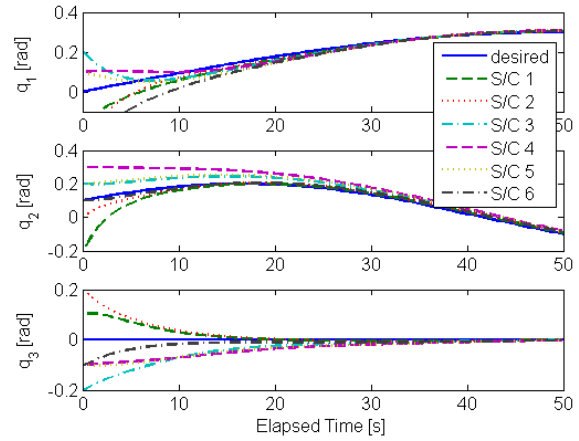
(a) proposed adaptive control with $\mathbf{K}_1'' = 60.0$ and $\mathbf{K}_2'' = 20.0$



(b) constant control with minimum control gains ($\mathbf{K}_1 = 60.0$ and $\mathbf{K}_2 = 20.0$)



(c) constant control with average control gains ($\mathbf{K}_1 = 237.7240$ and $\mathbf{K}_2 = 79.2413$)



(d) constant control with maximum control gains ($\mathbf{K}_1 = 250.9244$ and $\mathbf{K}_2 = 92.9140$)

Figure 5. State trajectories and relative errors with respect to q_1 by the proposed adaptive control and the constant control with three different control gains for the spacecraft formation flying system. The gains are chosen by the adaptive control gain information. (“S/C” denotes spacecraft.)

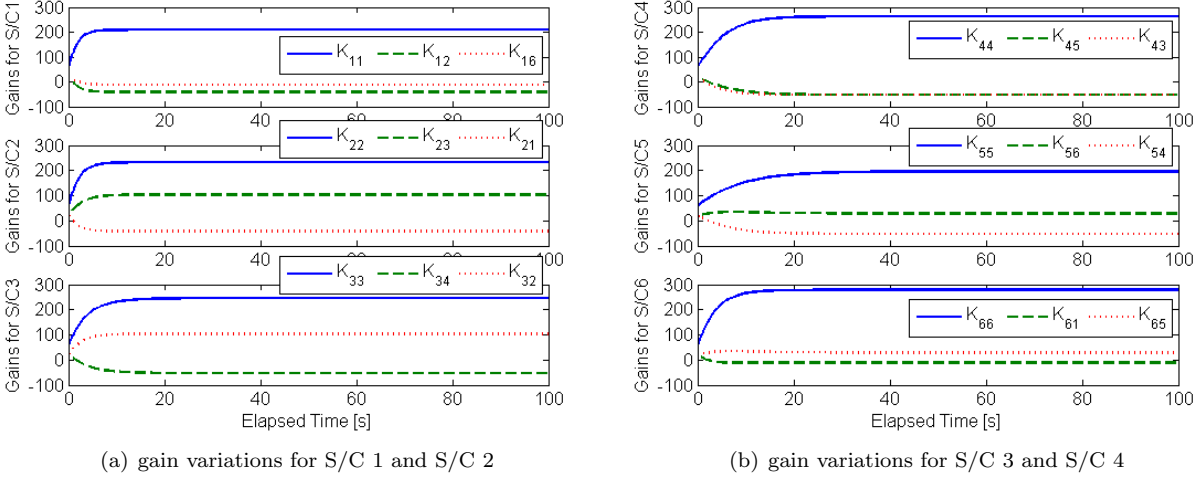


Figure 6. Time histories of the tracking control gains ($K_{ii} = K''_{ii} + K'_{ii}$) and the diffusive coupling gains ($K_{il} = K''_{il} + K'_{il}$ ($i \neq l$)) by the active parameter adaptation law in the proposed adaptive cooperative control for the spacecraft formation flying system. (“S/C” denotes spacecraft.)

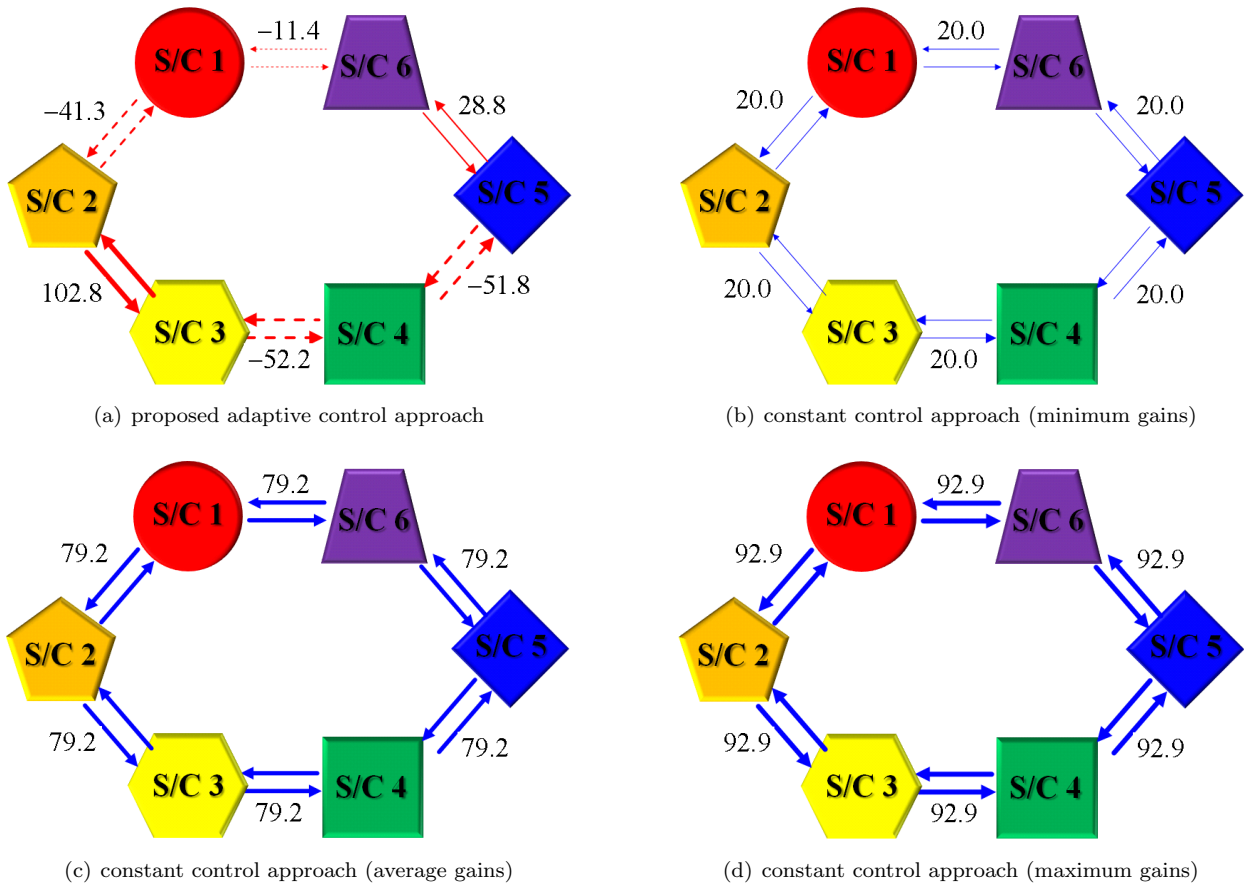


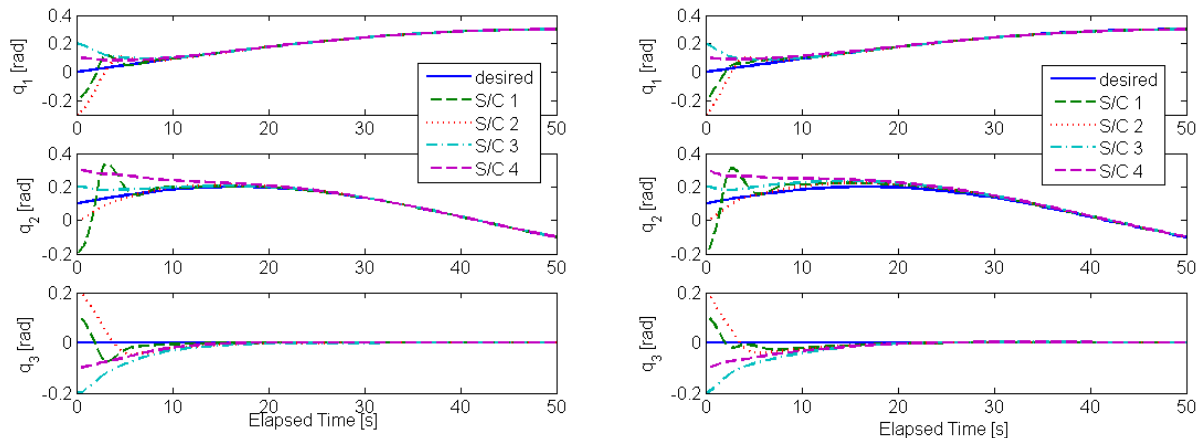
Figure 7. Comparison of the diffusive coupling gains in the simulation I by the proposed cooperative control ($K_{il} = K''_{il} + K'_{il}$ ($i \neq l$)) and the three different constant cooperative controls. The thickness of the arrows and the numbers beside them show the diffusive coupling gains between two spacecraft. Dashed lines denote negative values. (“S/C” denotes spacecraft.)

previously described in this section. For simulation, it is assumed that the initial guess of the moments of inertia ($\hat{\mathbf{J}}_i(0)$, $i = 1, 2, 3, 4$) is as follows:

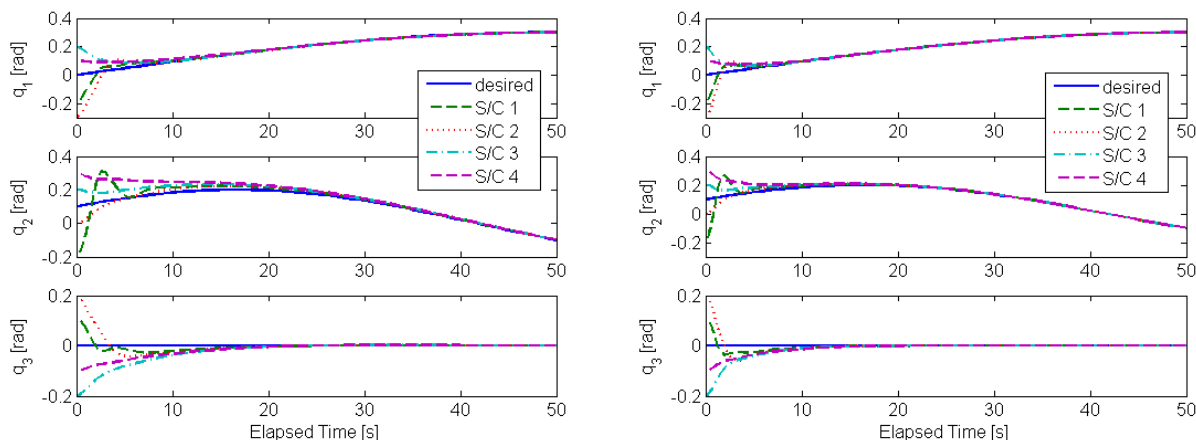
$$\hat{\mathbf{J}}_1(0) = 20\mathbf{I}_3, \quad \hat{\mathbf{J}}_2(0) = 2\hat{\mathbf{J}}_1(0), \quad \hat{\mathbf{J}}_3(0) = 3\hat{\mathbf{J}}_1(0), \quad \text{and} \quad \hat{\mathbf{J}}_4(0) = 4\hat{\mathbf{J}}_1(0)$$

where \mathbf{I}_3 denotes the 3×3 identity matrix.

All other values for the simulation are assumed to be the same as those in Simulation I.



(a) proposed adaptive control with $\mathbf{K}_1'' = 60.0$ and $\mathbf{K}_2'' = 20.0$ (b) constant control with average control gains ($\mathbf{K}_1 = 168.9876$ and $\mathbf{K}_2 = 56.3292$)



(c) constant control with maximum control gains ($\mathbf{K}_1 = 174.3523$ and $\mathbf{K}_2 = 58.1174$) (d) constant control with special control gains ($\mathbf{K}_1 = 365.4$ and $\mathbf{K}_2 = 121.8$)

Figure 8. State trajectories by the proposed adaptive control and the constant control with three different control gains for the spacecraft formation flying system with hybrid cooperative control. The gains are chosen by the adaptive control gain information.

Figure 8 shows the state trajectories of the proposed hybrid adaptive cooperative control and the three different constant cooperative controls (average, maximum, and special control gains). The average and the maximum control gains are obtained in the same way as mentioned in the previous simulation. The special control gain is the value for making similar convergent time to that of the proposed hybrid adaptive cooperative control (Table 3). The overall shapes of the state trajectories by the proposed hybrid adaptive cooperative control and the constant cooperative controls in Figure 8 are similar. This is because the difference of the values between the average control gain and the maximum control gain is small. Table 3 shows the simulation results about convergent time and total angular momentum changes. It should be noted that the convergence criterion ($|\mathbf{q}| \leq 0.002$ rad, $\forall \mathbf{q}$) for this simulation is different from that for the previous simulation ($|\mathbf{q}| \leq 0.001$ rad, $\forall \mathbf{q}$). Because of the effect by the unknown parameters, the convergent

Table 3. Convergent time (t at $|\mathbf{q}| \leq 0.002$ rad, $\forall \mathbf{q}$) and total angular momentum changes by the adaptive control and the constant controls with three different conditions (average ($\mathbf{K}_1 = 168.9876$ and $\mathbf{K}_2 = 56.3292$), maximum ($\mathbf{K}_1 = 174.3523$ and $\mathbf{K}_2 = 58.1174$), and special values for similar convergent time ($\mathbf{K}_1 = 365.4$, $\mathbf{K}_2 = 121.8$)) for the spacecraft formation flying system

	Adaptive control	Constant control		
		Average gains	Maximum gains	Special gains
Convergent time [s]	34.99	185.16	184.44	35.37
Angular momentum [Nms]	129.81	146.49	150.91	251.35

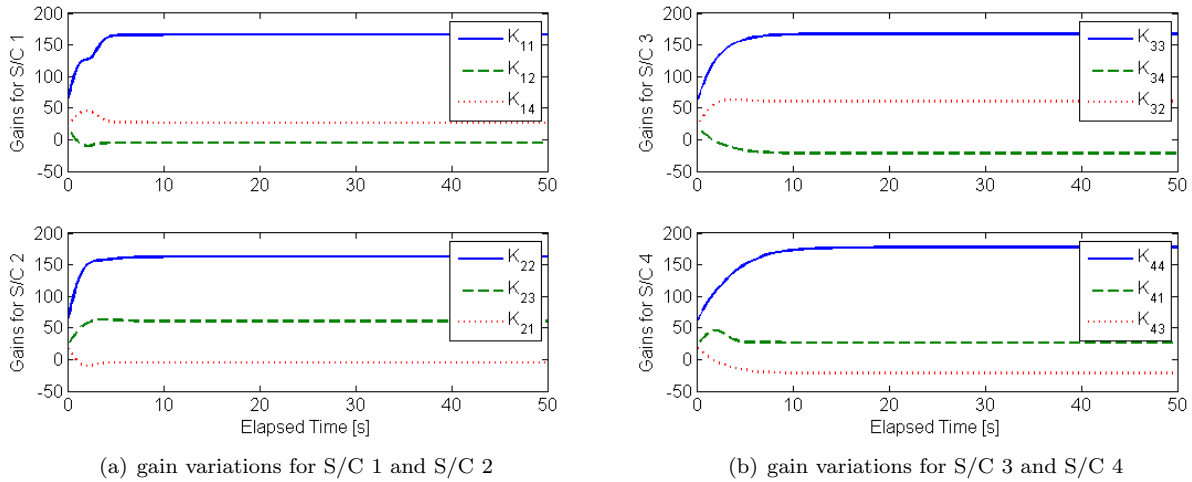


Figure 9. Time histories of the tracking control gains ($\mathbf{K}_{ii} = \mathbf{K}''_{ii} + \mathbf{K}'_{ii}$) and the diffusive coupling gains ($\mathbf{K}_{il} = \mathbf{K}''_{il} + \mathbf{K}'_{il}$ ($i \neq l$)) by the hybrid adaptive cooperative control for the spacecraft formation flying system

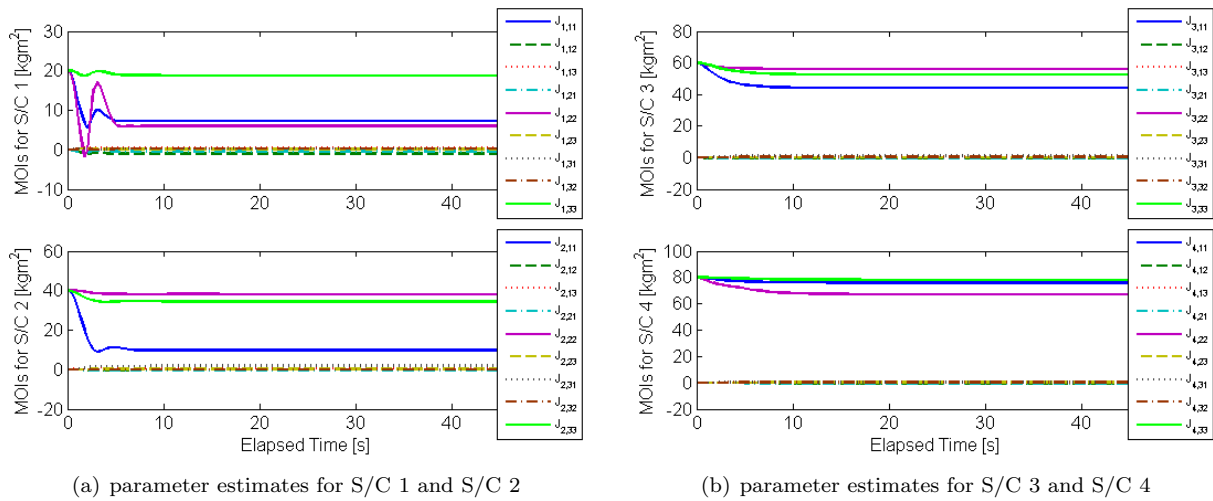


Figure 10. Time histories of the parameter estimates (moments of inertia for each spacecraft) by the hybrid adaptive cooperative control for the spacecraft formation flying system.

time with the same criterion is much longer than that of Simulation I. From Table 3, the automatically calculated control gains in Figure 9 make the convergent time of the proposed adaptive cooperative control much shorter than those of the constant cooperative controls with the average and maximum control gains. The constant control approach with the special gain has almost same convergent time as that of the proposed adaptive cooperative control, while the total angular momentum change is found to increase by more than 93%. Figure 10 shows the parameter estimation in the proposed hybrid adaptive cooperative control. The values in the figures are efficiently estimated by the cooperation with the active parameter adaptation law.

From the simulation results from the linear cart system and the spacecraft formation flying system, we could evaluate the performance of the proposed adaptive cooperative control and the proposed hybrid adaptive cooperative control. The results show the reliability of the proposed adaptive control approach. That is, the proposed adaptive control approaches are not sensitive to the initial control gains, which are usually selected by the system designers, while the performance by the constant cooperative control is significantly affected by the tracking control and diffusive coupling gains. This shows the superiority of the proposed adaptive cooperative control approaches.

VI. Conclusions

We presented a new adaptive cooperative control strategy for heterogeneous robotic networks inspired by the biological adaptive immune system. The dynamic models are described by using the Lagrangian formulation, which can be straightforwardly extended to linear and double integrator dynamics. The nonlinear stability of the complex dynamic network system is proven by employing contraction analysis. The key stability results indicate that the controlled system is globally asymptotically synchronized. The proposed adaptive cooperative control actively adapts system parameters based on tracking errors of individual robots and synchronization errors from interaction with neighbors. Unlike some prior work,⁴ which used only fixed control gains for satisfying the stability condition of the modified Laplacian matrix, the proposed adaptive control law achieves the flexibility of opportunistic gain selection as well as the optimality of adaptive control. As a result, we can avoid a degradation of control performance that arises from the heterogeneity of the network. Moreover, the proposed adaptive cooperative control can be applied to any network structure. We applied the proposed adaptive cooperative control to coupled linear cart systems and heterogeneous formation flying spacecraft to evaluate the reliability and superiority of the proposed adaptive cooperative control. Moreover, the proposed hybrid adaptive cooperative control shows the applicability to systems with unknown parameters. Simulation results show the effectiveness of the proposed method especially when the unknown environmental factors cannot be easily quantified or measured.

Acknowledgments

This was supported by the Air Force Office of Scientific Research (AFOSR). The authors thank Prof. James Oliver at the Virtual Reality Application Center, Iowa State University for his support. The authors gratefully acknowledge stimulating discussions with Prof. Jean-Jacques E. Slotine at Massachusetts Institute of Technology.

References

- ¹J. A. Bluestone and A. K. Abbas, "Natural Versus Adaptive Regulatory T Cells", *Nature Reviews Immunology*, Vol. 3, 2003, pp. 253–257.
- ²I. Chang, S.-Y. Park, and K.-H. Choi, "Decentralized Coordinated Attitude Control for Satellite Formation Flying via the State-Dependent Riccati Equation Technique," *International Journal of Non-Linear Mechanics*, (in Press) [DOI: 10.1016/j.ijnonlinmec.2009.06.001].
- ³I. Chang, S.-Y. Park, and K.-H. Choi, "Nonlinear Attitude Control of a Tether-Connected Multi-Satellite System in Three-Dimensional Free Space," *IEEE Transactions on Aerospace and Electronic Systems*, (in Press).
- ⁴S.-J. Chung and J.-J. E. Slotine, "Cooperative Robot Control and Concurrent Synchronization of Lagrangian Systems," *IEEE Transactions on Robotics*, Vol. 25, No. 3, 2009, pp. 686–700.
- ⁵S.-J. Chung, U. Ahsun, and J.-J. E. Slotine, "Application of Synchronization to Formation Flying Spacecraft: Lagrangian Approach," *Journal of Guidance, Control and Dynamics*, Vol. 32, No. 2, 2009, pp. 512–526.
- ⁶M. S. de Queiroz, V. Kapila, and Q. Yan, "Adaptive Nonlinear Control of Multiple Spacecraft Formation Flying", *Journal of Guidance, Control, and Dynamics*, Vol. 23, No. 3, 2000, pp.385–390.
- ⁷J. A. Fax and R. M. Murray, "Information Flow and Cooperative Control of Vehicle Formations," *IEEE Transactions*

on *Automatic Control*, Vol. 49, No. 9, 2004, pp. 1465–1476.

⁸A. Jadbabaie, J. Lin, and A. S. Morse, “Coordination of Groups of Mobile Autonomous Agents Using Nearest Neighbor Rules,” *IEEE Transactions on Automatic Control*, Vol. 48, No. 6, 2003, pp. 988–1001.

⁹J. Jouffroy and J.-J. E. Slotine, “Methodological Remarks on Contraction Theory,” *IEEE Conference on Decision and Control*, Atlantis, Paradise Island, Bahamas, 2004.

¹⁰K. Krstić and H. Deng, *Stabilization of Nonlinear Uncertain Systems*, Springer-Verlag, New York, NY, 1998.

¹¹Z. Lin, M. Broucke, and B. Francis, “Local Control Strategies for Groups of Mobile Autonomous Agents,” *IEEE Transactions on Automatic Control*, Vol. 49, No. 4, 2004, pp. 622–629.

¹²W. Lohmiller and J.-J. E. Slotine, “On Contraction Analysis for Nonlinear Systems,” *Automatica*, Vol. 34, No. 6, 1998, pp. 683–696.

¹³W. Luo, Y. -C. Chu, and K. -V. Ling, “Inverse Optimal Adaptive Control for Attitude Tracking of Spacecraft,” *IEEE Transactions on Automatic Control*, Vol. 50, No. 11, 2005, pp. 1639–1654.

¹⁴R. M. May, S. Gupta, and A. R. McLean, “Infectious Disease Dynamics: What Characterizes a Successful Invader?” *Philosophical Transactions of the Royal Society B. Biological Sciences*, Vol. 356, No. 1410, 2001, pp. 901–910.

¹⁵M. Mesbahi and F. Y. Hadaegh, “Formation Flying of Multiple Spacecraft via Graphs, Matrix Inequalities, and Switching,” *Journal of Guidance, Control, and Dynamics*, Vol. 24, No. 2, 2001, pp. 369–377.

¹⁶R. M. Murray, “Recent Research in Cooperative Control in Multivehicle Systems”, *Journal of Dynamic Systems, Measurement, and Control*, Vol. 129, 2007, pp. 571–583.

¹⁷G. Niemeyer and J.-J. E. Slotine, “Telemanipulation With Time Delays,” *International Journal of Robotics Research*, Vol. 23, No. 9, 2004, pp. 873–890.

¹⁸M. A. Nowak and K. Sigmund, “Evolutionary Dynamics of Biological Games,” *Science*, Vol. 303, No. 5659, 2004, pp. 793–799.

¹⁹R. Olfati-Saber and R. M. Murray, “Consensus Problems in Networks of Agents with Switching Topology and Time-Delays,” *IEEE Transactions on Automatic Control*, Vol. 49, No. 9, 2004, pp. 1520–1533.

²⁰L. E. Parker, “Current State of the Art in Distributed Autonomous Mobile Robotics,” *International Symposium on Distributed Autonomous Robotic Systems (DARS)*, 2000.

²¹L. Ren, J. K. Mills, and D. Sun, “Adaptive Synchronized Control for a Planar Parallel Manipulator: Theory and Experiments”, *Journal of Dynamic Systems, Measurement, and Control*, Vol. 128, 2006, pp. 976–979.

²²W. Ren, R. W. Beard, and E. Atkins, “Information Consensus in Multivehicle Cooperative Control,” *IEEE Control Systems Magazine*, Vol. 27, No. 2, 2007, pp. 71–82.

²³S. Shrestaa, C. T. Phama, D. A. Thomasa, T. A. Grauberta, and T. J. Ley, “How Do Cytotoxic Lymphocytes Kill Their Targets?” *Current Opinion in Immunology*, Vol. 10, No. 5, 1998, pp. 581–587.

²⁴J.-J. E. Slotine, “Modular Stability Tools for Distributed Computation and Control,” *International Journal of Adaptive Control and Signal Processing*, Vol. 17, No. 6, 2003, pp. 397–416.

²⁵J.-J. E. Slotine and W. Li, *Applied Nonlinear Control*, Prentice Hall, NJ, 1991.

²⁶J.-J. E. Slotine, personal communication with Prof. J.-J. E. Slotine, December 2007.

²⁷D. J. Stilwell and B. E. Bishop, “Platoons of Underwater Vehicles,” *IEEE Control Systems Magazine*, Vol. 20, No. 6, 2000, pp. 45–52.

²⁸D. M. Stipanović, G. İnalhan, R. Teo, and C. J. Tomlin, “Decentralized Overlapping Control of a Formation of Unmanned Aerial Vehicles,” *Automatica*, Vol 40, 2004, pp. 1285–1296.

²⁹D. Sun and J. K. Mills, “Adaptive Synchronized Control for Coordination of Multi-Robot Assembly Tasks,” *IEEE Transactions on Robotics and Automation*, Vol. 18, No. 4, 2002, pp. 498–510.

³⁰İ. Uzman, R. Burkan, and H. Sarikaya, “Application of Robust and Adaptive Control Techniques to Cooperative Manipulation”, *Control Engineering Practice*, Vol. 12, No. 2, 2004, pp. 139–48.

³¹W. Wang and J.-J. E. Slotine, “A Theoretical Study of Different Leader Roles in Networks,” *IEEE Transactions on Automatic Control*, Vol. 51, No. 7, 2006, pp. 1156–1161.

³²J. D. Wolfe, D. F. Chichkat, and J. L. Speyer, “Decentralized Controllers for Unmanned Aerial Vehicle Formation Flight,” *AIAA Guidance, Navigation, and Control Conference*, San Diego, CA, 1996, AIAA Paper 96-3833.